On the contribution of remote sensing-based calibration to model multiple hydrological variables

A. M. Oliveira[1], A. S. Fleischmann[1], and R. C. D. Paiva[1]

[1] Instituto de Pesquisas Hidráulicas (IPH), Universidade Federal do Rio Grande do Sul – UFRGS, Av. Bento Gonçalves, 9500, Porto Alegre 90050-260, RS, Brazil.

Corresponding author: Aline Meyer Oliveira (alinemey@gmail.com)

Key Points:

- Calibration/evaluation of a hydrological-hydrodynamic model with five remote sensing-based water cycle variables in the Amazon region
- Different calibration strategies with remotely-sensed observations were able to improve water cycle representation
- Model calibration with multiple remotely sensed variables highlighted deficiencies in model structure and parameterization, and observations.

Abstract

The accuracy of hydrological model predictions is limited by uncertainties in model structure and parameterization, and observations used for calibration, validation and model forcing. While calibration is usually performed with discharge estimates, the internal model processes might be misrepresented, and the model might be getting the "right results for the wrong reasons", thus compromising model reliability. An alternative is to calibrate model parameters with remote sensing (RS) observations of the water cycle. Previous studies highlighted the potential of RS-based calibration to improve discharge estimates, focusing less on other variables of the water cycle. In this study, we analyzed in detail the contribution of five RS-based variables (water level (h), flood extent (A), terrestrial water storage (TWS), evapotranspiration (ET) and soil moisture (W)) to calibrate a coupled hydrologic-hydrodynamic model for a large Amazon sub-basin with extensive floodplains. Single-variable calibration experiments with all variables were able to improve discharge KGE from around 6.1% to 52.9% when compared to a priori parameter sets. Water cycle representation was improved with multi-variable calibration: KGE for all variables were improved in the evaluation period. By analyzing different calibration setups, a consistent selection of complementary variables for model calibration resulted in a better performance than incorporating all RS variables into the calibration. By looking at multiple RS observations of the water cycle, inconsistencies in model structure and parameterization were found, which would remain unknown if only discharge observations were considered.

Plain Language Summary

Hydrological models are important tools for many applications in water resources, such as natural hazards management, quantification of impacts of climate change or anthropogenic effects on the water cycle. However, there are uncertainties in these models, which might lead to inaccurate predictions. In many cases, they are related to calibrating parameters of the model by comparing in-situ streamflow observations with modeled streamflow estimates. Therefore, internal processes in the model might be misrepresented, i.e., the model might be getting the "right results for the wrong reasons", which compromises model reliability and its estimates. An alternative is to calibrate the model parameters with remote sensing (RS) observations of the water cycle. In this study, we analyzed the contribution of five RS-derived variables (water level, flood extent, terrestrial water storage, evapotranspiration, and soil moisture) to calibrate model parameters. We found that RS-based calibration was able to improve water cycle representation (e.g., calibration with water level was able to improve estimates of water level, flood extent, terrestrial water storage and evapotranspiration). Moreover, by looking at multiple RS observations of the water cycle, we were able to found inconsistencies in model structure and parameterization, which would remain unknown if only discharge observations were considered.

1 Introduction

The accurate representation of hydrologic processes in mathematical models remains a key challenge in water resources research and applications (Baroni et al., 2019; Clark et al., 2015; Kirchner, 2006; Nearing et al., 2016; Semenova & Beven, 2015) due to uncertainties in model structure (Wagener et al., 2003), parameterization (Gharari et al., 2014; Shafii & Tolson, 2015), and observations (Di Baldassarre & Montanari, 2009). These uncertainties might lead to inaccurate predictions of hydrological variables for water resources and natural hazards management (Grimaldi et al., 2019; Montanari & Koutsoyiannis, 2014), and for quantification of impacts of climate change and anthropogenic effects on the water cycle (Haddeland et al., 2006; Teutschbein & Seibert, 2012; C. Y. Xu et al., 2005). This problem has led for instance to initiatives to better constrain the terrestrial water budget by fusing models and Earth Observation datasets (M. Pan & Wood, 2006; Pellet et al., 2019).

Traditionally, hydrological models are calibrated against gauged streamflow data, which might hamper predictions in ungauged sites, since it does not guarantee an accurate representation of other water cycle components (e.g., soil moisture and evapotranspiration), thus leading to uncertainty in hydrologic predictions (Hrachowitz et al., 2013). Moreover, many parameter sets can provide equally acceptable performances for streamflow evaluation (i.e., the equifinality thesis), but they might be "right for the wrong reasons" (Beven, 2006; Kirchner, 2006). Several solutions have been proposed to improve process representation and reduce uncertainty in model predictions, such as the generalized likelihood uncertainty estimation (Beven & Binley, 1992), dynamic

identifiability analysis (Wagener et al., 2003), multiscale parameter regionalization (Samaniego et al., 2010), and multi-objective calibration (Yapo et al., 1998). However, these are ongoing developments, and stand out as one of the twenty-three unsolved problems in hydrology (Blöschl et al., 2019): "how can we disentangle and reduce model structural/parameter/input uncertainty in hydrological prediction?".

In addition to the presented solutions, an alternative is the use of complementary datasets besides streamflow observations for model calibration (e.g., Crow et al., 2003; Franks et al., 1998; Lo et al., 2010; López et al., 2017; Rajib et al., 2016), data assimilation (e.g., Brêda et al., 2019; Houser et al., 1998; Mitchell et al., 2004; Paiva et al., 2013; Pathiraja et al., 2016; Reichle et al., 2002; Vrugt et al., 2005), or validation (e.g., Alkama et al., 2010; Motovilov et al., 1999; Neal et al., 2012; Siqueira et al., 2018). Such approaches are promising to improve representation of processes in hydrological models (Clark et al., 2015), reduce uncertainty in hydrological predictions (Gharari et al., 2014), understand equifinality (Beven, 2006), and perform predictions in ungauged or poorly-gauged sites (Sivapalan et al., 2003). However, distributed data of complementary hydrological variables (e.g., evapotranspiration, soil moisture) are scarce, and in-situ measurements present poor spatial and temporal representativeness.

In this context, remote sensing (RS) observations have stood out in the last decade because of their increasing spatial and temporal resolutions, free availability in many cases, and capability to record less monitored hydrological variables such as soil moisture, evapotranspiration, and terrestrial water storage (Lettenmaier et al., 2015). For instance, GRACE mission provided monthly estimates of changes in water storage on a global coverage with an accuracy of 2 cm when uniformly estimated over land and oceans (Tapley et al., 2004). Missions such as SMOS, SMAP, AMSR-E and ASCAT were estimated to provide soil moisture data with a median RMSE of 0.06-0.10 m^3/m^3 for the CONUS (Karthikeyan et al., 2017). Altimeters such as Envisat, Jason-2 and ICESat-1 and ICESat-2 can yield water level data with an accuracy ranging from 0.04 m to 0.42 m, involving trade-offs between temporal resolution from 10 to 91 days, and cross-track separation from 15 to 315 km (Jarihani et al., 2013), while the future SWOT mission will provide at least one water level measurement every 21 days for global rivers wider than 100 m (Biancamaria et al., 2016).

Although previous studies have analyzed the value of integrating RS data into hydrological modeling through calibration or data assimilation (see review by Xu et al., 2014 and Jiang & Wang, 2019), this topic has not been fully explored to its potential yet. Therefore, in section 1.1, we present major knowledge gaps in the context of RS-based calibration of hydrological models through an extensive literature review. In section 1.2, we describe the aims and contributions of this study.

1.1 Literature review on calibration of hydrological models with RS data

A comprehensive, yet non-exhaustive literature review of studies that used RS datasets for parameter estimation in hydrological models is presented in this section and summarized in Figure 1. A total of 62 research articles was found (Supporting

Information Table S1). Most publications involved large study areas (> 1000 km²), which is expected because of the usual coarse resolution of RS products. Most studies used RS-derived evapotranspiration for model calibration, followed by soil moisture (Figure 1b), but there were also attempts for calibration of up to eight different RS-derived variables (Nijzink et al., 2018). This indicates a still existent knowledge gap regarding which RS-derived variables are more useful for model calibration. Indeed, many recent studies have investigated the added value of RS-derived information to calibrate hydrological models (Figure 1d; Table S1).

Most of the studies (69.35%) used only one RS product for model calibration (Figure 1e, in black), while twelve studies (19.35%) used two products, and five (8.06%) used three products. Only few studies used more than three RS products for model calibration (Demirel et al., 2019; Nijzink et al., 2018). Some studies addressed the use of RS data to estimate discharge in ungauged basins (Kittel et al., 2018; Sun et al., 2010), while others focused on narrowing the parameter search space, and thus equifinality reduction, by combining multiple variables for calibration (e.g., Nijzink et al., 2018; Pan et al., 2018). This is confirmed by Figure 1e (in blue), which demonstrates that the vast majority of researches used two variables for calibration (in general, discharge and a RS-derived variable). Within these studies, some analyzed model performance in terms of discharge only, while others considered different variables (Figure 1e, in red), providing a more comprehensive discussion on inconsistencies of hydrological models (e.g., Koch et al., 2018; Li et al., 2018).

Regarding how RS is incorporated into the model calibration procedure (Figure 1h), 65.6% of the articles used RS-based spatially distributed information, thus calibrating the model with distributed objective functions (e.g., pixel-by-pixel or by sub-basin). Within these studies, bias-insensitive functions have been recently introduced (e.g., Koch et al., 2018; Demirel et al., 2018; Zink et al., 2018; Dembele et al., 2020), being important for reducing the impact of RS data uncertainty on the parameter estimation procedure. The remaining publications (34.4%) incorporated RS data as an average for the whole basin.

Finally, there is still a need for more studies in tropical regions (especially South America) (Figure 1c), which have particular hydro-climatic characteristics, and so have different requirements than temperate regions on model process representation (e.g., snow-related processes might not be so relevant in some tropical areas, whereas an accurate representation of floodplains might be). In the case of basin with complex river-floodplain interactions as in the Amazon, an accurate flood wave routing method is required to correctly depict the water transport along the drainage network. Our analysis shows that most studies used simple flood wave routing schemes such as kinematic wave or Muskingum (Figure 1g). Only 10.4% attempted to couple hydrologic and river hydrodynamic models, highlighting the necessity of better understanding the applicability of RS-based calibration in basins with major flat regions with wetlands (Hodges, 2013; Neal et al., 2012; Pontes et al., 2017).

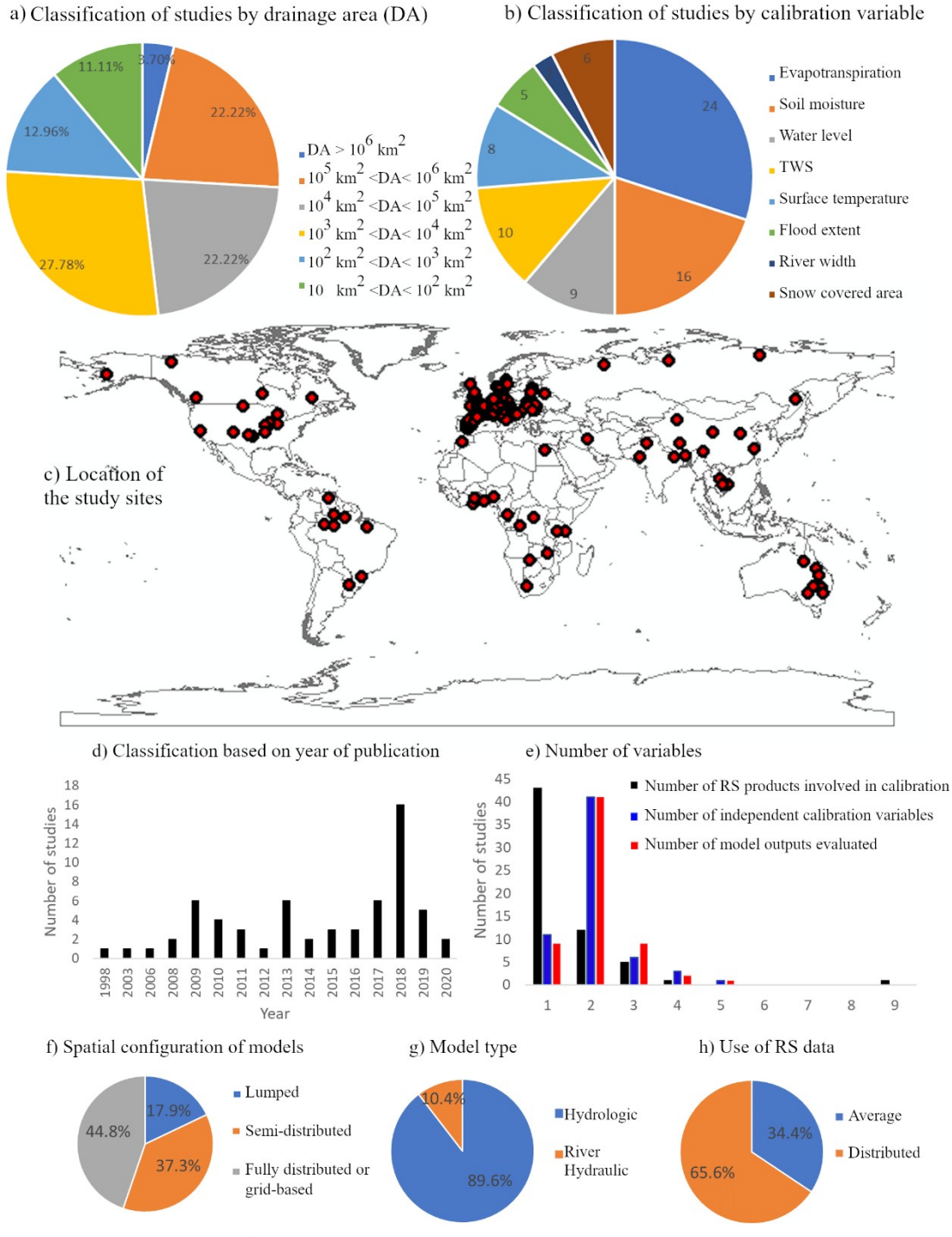

Figure 1. Summary of the literature review on 62 studies that incorporated RS datasets for parameter estimation in hydrological models (see Table S1 in Supporting Information). (a) Classification of publications based on the drainage area of study sites (an average value was considered for publications that used multiple study sites); (b) distribution of studies based on the calibration variable; (c) geographical distribution of study sites; (d) number of publications per year; (e) number of RS products involved in calibration (in black), number of independent calibration variables (in blue), and number of model outputs evaluated (in red); (f) classification of models based on their spatial configuration; (g) model type; and (h) use of RS data

1.2 Aims and Contributions of this paper

Our study addresses major knowledge gaps identified in the previous literature review in the context of RS-based calibration of hydrological models. Firstly, most of the studies analyzed two or less variables (Figure 1e). Here, we used RS observations of a large number of variables for model calibration, namely soil moisture, evapotranspiration, terrestrial water storage, flood extent and river water levels, and thus move beyond the contributions of RS for improving only discharge estimates. By simultaneously looking at different variables, we also move towards an improved representation of the water cycle as a whole, enhancing our ability to identify model limitations and inconsistencies. Furthermore, most studies to date focused on European, temperate watersheds (Figure 1c), which largely differ from tropical basins in terms of hydroclimatic characteristics and river-wetland interactions. In this context, large-scale, coupled hydrologic-hydrodynamic models have faced major developments in recent years (Yamazaki et al 2011, Paiva et al 2013, Fleischmann et al 2020), but to our knowledge the complementarity of hydrologic (soil moisture, evapotranspiration, terrestrial water storage) and hydrodynamic (flood extent and river water level) RS observations for model calibration has not yet been addressed in the literature. Here we present a study case in a tropical basin with extensive floodplains in the Amazon with a state-of-the-art coupled hydrologic-hydrodynamic model, which together with the previously mentioned advances provide important contributions to the growing literature of RS-based calibration of hydrological models.

2 Methods

2.1 Experimental design

A hydrological-hydrodynamic model (MGB; (Collischonn et al., 2007)) is set up for a case study in the Amazon (Purus River Basin) with a priori parameter sets based on their variability as reported in literature (references in Table S2). The study is then divided into two steps.

Firstly, a sensitivity analysis is performed to understand how different parameter sets (river hydraulic, soil, vegetation) affect model output variables (river discharge, flood extent, river water level, soil moisture, evapotranspiration and terrestrial water storage).

Then, a calibration step is performed in which the model is calibrated with the well-known MOCOM-UA optimization algorithm (Yapo et al., (1998)) considering six variables: (1) in-situ streamflow (one gauge at the basin outlet), and RS freely available, state-of-the-art observations of (2) water level (one satellite altimetry virtual station), (3) flood extent (sum of flooded areas over the Lower Purus River Basin), (4) terrestrial water storage (TWS), (5) evapotranspiration, and (6) soil moisture. Variables (4), (5) and (6) are averaged over the whole basin. The calibration of each variable is performed

individually (single-variable), and evaluated for all variables. All calibration experiments are repeated three times with differing initial parameter sets to ensure that convergence is not dependent on the initial parameter sets. Given limitations on the availability of simultaneous RS time coverage, the model is calibrated for one time period (2009-2011), and evaluated for: (i) the same time period of calibration; and (ii) for a different period (2006–2008 for discharge, flood extent, TWS, ET and 2013–2014 for water level and soil moisture). To understand how lumped calibration can retrieve the remotely sensed spatial patterns, a qualitative evaluation is provided additionally. A final test is performed in which two multi-variable calibration experiments are conducted: (i) calibration with all analyzed variables, except discharge; and (ii) calibration with two complementary variables (water level and soil moisture), which are selected for simultaneous calibration for being complementary and having led to satisfactory calibration performance.

2.2 Study area: Purus River Basin

The Purus River Basin (Figure 2) in Amazon has a drainage area of approximately 236,000 km², and river discharge ranges from around 1,000 (June-December) to 12,000 m³/s (January-July) at Canutama gauge. Because of its large area, it is compatible with the spatial resolution of RS products (e.g., a pixel of GRACE presents spatial resolution of roughly 300-400 km). Purus river has minor anthropogenic influences, which simplifies the modeling process. The climate is equatorial (Figure 2d), and mean annual rainfall is 2147 mm/year (according to in-situ gauges). Purus was selected because of its representativeness of tropical regions as the Amazon basin, which is the largest river in the world (Holeman, 1968), and it is characterized by extensive floodplains (Junk, 1997). For instance, on the lower Purus, the floodplain width is in the order of 30 km, which corresponds to approximately 30 times the main channel width (Paiva et al., 2011). These floodplains allow a satisfactory flood extent monitoring by RS image classification, which contributes to the suitability of Purus River Basin for this study.

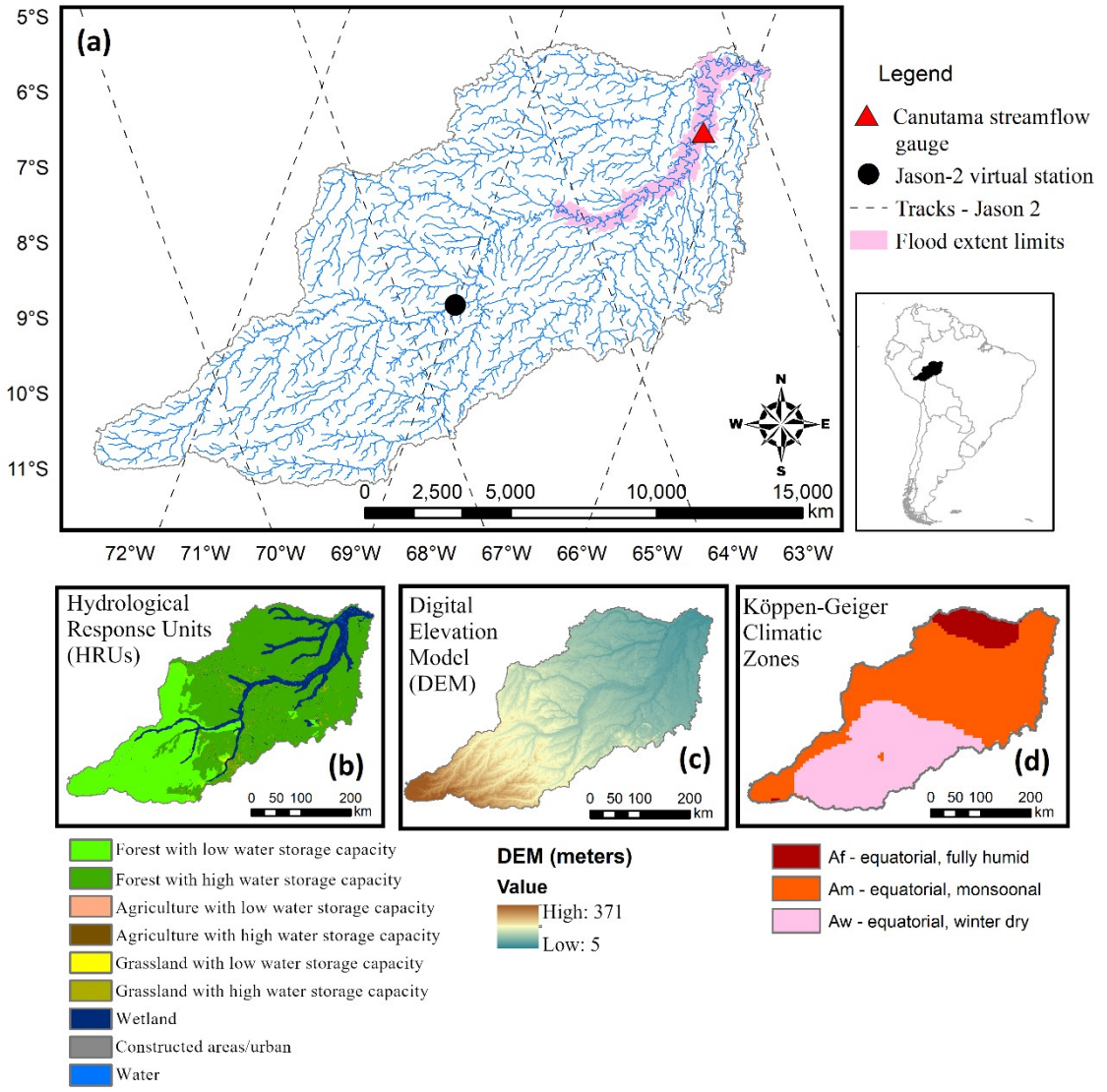

Figure 2. Study area: Purus River Basin. (a) drainage network (in blue), location of the discharge gauge (Canutama, triangle in red), tracks of the spatial altimetry mission Jason 2 (dashed black lines), location of the altimetry virtual station (circle, in black), and the area used for extraction of flood extent (Lower Purus, pink polygons); (b) Hydrological Response Units (Fan et al., 2015); (c) Bare Earth Digital Elevation Model (O'Loughlin et al., 2016); (d) Köppen-Geiger Climatic Zones (Kottek et al., 2006).

2.3 Hydrological-hydrodynamic model: MGB

The MGB ("Modelo de Grandes Bacias", a Portuguese acronym for "Large Basin Model") is a semi-distributed, hydrological-hydrodynamic model (Collischonn et al., 2007; Pontes et al., 2017). It was chosen for this study because (1) it has been widely and successfully applied in several South American basins (e.g., Paiva et al., 2013; Siqueira et al., 2018); (2) it is representative and similar to other conceptual hydrological models like VIC (Liang et al., 1994) and SWAT; and (3) the hydrological component is tightly coupled to a hydrodynamic routing scheme, allowing the

265 simulation of complex flat, tropical basins. Moreover, the source code of MGB is freely
266 available at www.ufrgs.br/lsh.

267 Within the model structure, basins are discretized into unit-catchments, which are
268 further divided into Hydrological Response Units (HRU's) based on soil type and land
269 use. A vertical water balance is performed for each HRU, considering canopy
270 interception, soil infiltration, evapotranspiration, and generation of surface, subsurface
271 and groundwater flows. Soil is represented as a bucket model with a single layer. Flow
272 generated in each HRU is routed to the outlet of the unit-catchment with linear
273 reservoirs. Outflow from each unit-catchment is then propagated through the stream
274 network by using a 1D hydrodynamic model based on the inertial approximation
275 proposed by Bates et al. (2010). The stream network is derived from Digital Elevation
276 Model (DEM) processing. The model has 19 parameters, which are further detailed in
277 the next section. Other model inputs are precipitation, climate data, soil type and land
278 use maps, which are further described in section *2.6 Model Setup.*

279

280 **2.4 A priori uncertainty of model parameters**
281

282 Within MGB model, there are parameters related to vegetation cover (albedo, leaf area
283 index, vegetation height and Penman-Monteith surface resistance), river hydraulics
284 (Manning's roughness, and width and depth parameters related to geomorphological
285 relationships), and conceptual parameters related to soil water budget (Wm, b, Kbas,
286 Kint, XL, CAP, Wc, CI, CS, CB), which are further detailed in Supporting Information
287 (Table S2). Out of the 19 model parameters, six are fixed and 13 are calibrated.

288 The a priori uncertainty of MGB model parameters is estimated based on their
289 variability as reported in literature (references in Table S2). Supporting Information
290 (Table S2) presents the calibration parameters, their initial values, range, and the
291 references that support these assumptions.

292

293 **2.5 Sensitivity analysis**
294

295 In order to understand how different parameter sets (river hydraulic, soil, vegetation)
296 affect model output variables (river discharge, flood extent, river water level, soil
297 moisture, evapotranspiration and terrestrial water storage), multiple model runs were
298 conducted considering four uncalibrated model setups: (1) varying only soil parameters;
299 (2) varying only vegetation parameters; (3) varying only hydraulic parameters; (4)
300 varying all parameters together. One hundred runs were conducted in triplicate to ensure
301 that convergence is not dependent on the initial parameter sets, thus resulting in 300
302 runs for each setup. In this step, no RS-based calibration is performed yet.

303 Parameters were varied considering a uniform distribution, and results were analyzed in
304 terms of mean RMSD (root mean square deviation) of each variable, by comparing each
305 run with a reference one (i.e., the initial run with the initial parameter set as defined in

Supporting Information Table S2). This was performed in order to understand the sources of model uncertainties related to different sets of parameters (e.g., are flood extent estimates sensitive to vegetation parameters, or are ET estimates sensitive to hydraulic parameters?). The dispersion of model outputs was also compared to uncertainty in the observations, as derived from literature.

To understand which variables are inter-related in the model, we further analyzed the results of setup "(4) varying all parameters together". This was done by firstly computing the Kling-Gupta Efficiency metric (KGE; Gupta et al., (2009)) between the perturbed runs and a reference one (i.e., run with the initial parameter set) for each variable, and then calculating the Pearson correlation (r) between KGE values for each pair of variables (e.g., discharge and water level, discharge and flood extent, and so forth). This experiment is relevant to evaluate whether two variables get improved or get worsened together, or whether a variable improvement impacts on the deterioration of another. In other words, this approach allows to evaluate the correlation between the variables.

2.6 Model setup

The Bare Earth Digital Elevation Model (DEM; O'Loughlin et al., 2016) (Figure 2c) was used for stream network computation and basin discretization with the IPH-HydroTools GIS package (Siqueira et al., 2016). The original DEM resolution is 90 m, and it was resampled to 500 m to facilitate GIS processing. An upstream area threshold of 100 km^2 was adopted to delineate the drainage network, and unit-catchments were discretized by dividing the stream network into fixed reach length of 10 km, resulting in 2957 unit-catchments for the whole basin. Soil type and land cover maps were extracted from the HRU discretization developed by Fan et al. (2015) (Figure 2b): (1) deep and (2) shallow forested areas, (3) deep and (4) shallow agricultural areas, (5) deep and (6) shallow pasture, (7) wetlands, (8) semi-impervious areas, and (9) open water, where "deep soils" refer to soils with high water storage capacity, and "shallow soils" are those with low water storage capacity. In the Purus River Basin, 57.4% of the region is covered by forest with deep soils, 26.9% by forest with shallow soils, and 13.7% by wetlands (i.e., river floodplains). Daily precipitation data were derived from TMPA 3B42 (version 7), with spatial resolution of 0.25º x 0.25º (Huffman et al., 2007; available at: <https://gpm.nasa.gov/data-access/downloads/trmm>), and were interpolated with the nearest neighbor method for the centroid of each unit-catchment. Long term climate averages for mean surface air temperature, relative humidity, insolation, wind speed and atmospheric pressure were obtained from the Climatic Research Unit database (New et al., 2000; available at: <http://www.cru.uea.ac.uk/data>), at a spatial resolution of 10', and also interpolated with the nearest neighbor method.

2.7 Model calibration

The MOCOM-UA calibration algorithm (Yapo et al., 1998; Multi-objective global optimization for hydrologic models) was adopted due to its satisfactory performance when coupled with hydrological models (e.g., Collischonn et al., 2008; Maurer et al., 2009; Naz et al., 2014). MOCOM-UA is an evolutionary algorithm, based on SCE-UA (Duan et al., 1992), that simultaneously optimizes a model population with respect to different objective functions. The model population consists of randomly distributed points within the parameter search space, and it reflects the a priori uncertainty of model parameters. Here, the population size was set to 100 individuals. The altered model parameters and their respective ranges are described in Supporting Information Table S2. All calibration experiments are repeated three times with differing initial parameter sets to ensure that convergence is not dependent on the initial parameter sets.

Objective functions to be optimized depend on the calibration setup. In the single-variable calibration, for each variable, three objective functions (*OF*) that summarize the agreement between simulated and observed (RS) time-series are simultaneously optimized: Pearson correlation (r), ratio of averages ($\mu_{¿}/\mu_{obs}$), and ratio of standard deviations ($\sigma_{¿}/\sigma_{obs}$), which are associated to the individual terms of KGE metric. These 3 objective functions are depicted in Equations 1 to 3, where X denotes the assessed variables (Q, h, A, TWS, ET or W).

$$OF_1=\left(\frac{\mu_{¿}}{\mu_{obs}}\right)_X (1); OF_2=\left(\frac{\sigma_{¿}}{\sigma_{obs}}\right)_X (2); OF_3=r_X (3)$$

For the multi-variable calibration, the objective functions are the KGE of each variable considered: firstly, five objective functions were considered (KGE of all variables except discharge), as depicted in Equations 4 to 8.

$$OF_1=KGE_h (4); OF_2=KGE_A (5); OF_3=KGE_{TWS} (6); OF_4=KGE_{ET} (7); OF_5=KGE_W (8)$$

Secondly, two objective functions were adopted (KGE of selected variables 1 (x) and 2 (y)), as depicted in Equations 9 and 10.

$$OF_1=KGE_x (9); OF_2=KGE_y (10)$$

Results are expressed in terms of a Skill Score (S) (Equation 11; Zajac et al., 2017), in order to evaluate the improvement (or deterioration) in the representation of a variable when the model is calibrated with a given variable, compared to the uncalibrated setup.

$$S=\frac{KGE_{calibrated}-KGE_{initial}}{1-KGE_{initial}} (11)$$

$KGE_{calibrated}$ is the mean KGE resulting from running the model with the calibrated parameters. $KGE_{initial}$ is the mean KGE resulting from running the model with the a priori parameter sets.

2.8 Calibration/Evaluation Data

35
36
387 In the next paragraphs we introduce the data used for model calibration and evaluation,
388 as well as how MGB outputs were evaluated in comparison to them.

389 -*In-situ discharge measurements* were obtained from the Brazilian Water Agency
390 Hidroweb database (available at:
391 <http://www.snirh.gov.br/hidroweb/publico/apresentacao.jsf>), at the gauge
392 "Canutama" (code: 13880000; location: S ° 32' 20.04"; W 64° 23' 8.88"; drainage area:
393 236,000 km², period of data availability: 1973 to 2016). Uncertainty in discharge
394 observations can be estimated as ranging from 6.2% to 42.8% at the 95% confidence
395 level, with an average of 25.6% (Di Baldassarre & Montanari, 2009). Discharge was
396 evaluated on a daily basis.

397 - *Remotely sensed water level data* were obtained from Jason-2 mission, which presents
398 an orbit cycle of approximately 10 days, and tracks separated by approximately 300 km
399 at the equator (Lambin et al., 2010). It presents an accuracy of approximately 0.28 m
400 (Jarihani et al., 2013), and data are available since 2008. The virtual station presented in
401 Figure 1 corresponds to Track number 165. Processed data for this study were
402 downloaded from the Hydroweb/Theia database (available at: <http://hydroweb.theia-
403 land.fr>). Water level was computed in MGB at the unit-catchment associated to the
404 altimetry virtual station, being an advantage of using the hydrodynamic scheme for
405 flood routing instead of the Muskingum simplification. Simulated and RS water level
406 data were compared every 10 days in terms of anomaly (values subtracted from long
407 term average).

408 - *Satellite flood extent data* were derived from ALOS-PALSAR imagery, which
409 presents a ground resolution of 100 m (Rosenqvist et al., 2007). Images were
410 downloaded from Alaska Satellite Facility (available at: <https://www.asf.alaska.edu/>)
411 in processing level 1.5, which already presents geometric and radiometric corrections. A
412 3 x 3 median filter was used to remove speckle noise (Lee et al., 2014). Images were
413 classified into water (backscattering coefficient less than -14 dB), non-flooded forest
414 (between -14 dB and -6.5 dB), and flooded forest (higher than -6.5 dB) classes,
415 according to Hess et al. (2003) and Lee et al. (2014). The uncertainty of flood extent
416 estimates was estimated based on the RMSE between the resulting classification of this
417 study, and the dual-season mapping developed by Hess et al. (2003). Simulated and RS
418 flood extent data were compared for the pink area depicted in Figure 1, in order to avoid
419 spurious flood extent data in regions that are known to be not subject to flooding.
420 ALOS-PALSAR presents a recurrence cycle of 46 days (from 2006 to 2011), and flood
421 extent data were available and compared to MGB for 21 dates.

422 - *Satellite-based terrestrial water storage (TWS) anomalies* were extracted from
423 GRACE mission, launched in March 2002. GRACE provides monthly TWS estimates
424 based on anomalies in gravitational potential, at a resolution of 300-400 km, with a
425 uniform accuracy of 2 cm over the land and ocean regions (Tapley et al., 2004). TWS
426 anomalies were retrieved from three processing centers - GFZ (Geoforschungs Zentrum
427 Potsdam, Germany), CSR (Center for Space Research at University of Texas, USE),
428 and JPL (Jet Propulsion Laboratory, USA), available at <https://grace.jpl.nasa.gov/>,
429 and then the mean value based on the three products was averaged for the whole basin.
430 In MGB, TWS values were computed as the sum of water storage of all hydrological

compartments: river, floodplains, soil, groundwater and vegetation canopy. Simulated and RS-based TWS were compared in terms of anomaly (values subtracted from long term average) at a monthly time-scale.

- *Satellite-based evapotranspiration* estimates were retrieved from the MOD16 product, derived by an algorithm presented by Mu et al. (2011) based on the Penman-Monteith equation. The dataset covers the period 2000-2010 with a spatial resolution of 1 km for global vegetated land areas. Because of that, even though MGB evapotranspiration is calculated for flooded areas (open water evaporation in main channel and floodplains) and vegetation for water balance purposes, only the vegetation-ET output was compared to MOD16. MOD16 products are provided in 8-days, monthly and annual intervals. Monthly intervals were used here and averaged for the whole basin. Accuracy of MOD16 along the Amazon basin is estimated as 0.76 mm/day (Gomis-Cebolla et al., 2019). MOD16 data is available at: < https://www.ntsg.umt.edu/project/modis/mod16.php>. In MGB, evapotranspiration is computed via Penman-Monteith equation, based on the climate input variables.

- *Satellite-based soil moisture* is derived from the SMOS mission (Kerr et al., 2001), processed by the Centre Aval de Traitement des Données SMOS (CATDS), and downloaded in processing level 4, which combines lower level products with data from other sensors and modeling/data assimilation techniques. The daily L4 root zone soil moisture product at 0-1 m soil depth (Al Bitar et al., 2013) were used (available at: <https://www.catds.fr/Products/Available-products-from-CEC-SM/L4-Land-research-products>), and data from ascending and descending orbits were averaged for the whole basin. In MGB, soil moisture as a saturation degree was computed as the water in the soil compartment divided by the maximum water capacity of the soil (*Wm* parameter). Since MGB estimates saturation degree values for a soil bucket reservoir, SMOS values were rescaled for the range 0 - 100% according to the Min/Max Correction method described by Tarpanelli et al. (2013) and applied by some studies (e.g., Rajib et al., 2016; Silvestro et al., 2015), and them compared to MGB on a daily time-scale as an average for the whole basin.

3 Results and discussion

Results are structured as follows. Firstly, the sensitivity analysis is presented with discussions on model uncertainties (Section 3.1). Then, results for model calibration are presented, with discussions on how RS-based model calibration can improve discharge and the water cycle representation as a whole (Section 3.2).

3.1 Sensitivity analysis

A sensitivity analysis was carried out to understand how different parameter types (river hydraulic, soil, vegetation, and all together) affect the variation of different hydrological processes in MGB (Figure 3a). This was performed by analyzing the dispersion of six

output variables (discharge, water level, flood extent, TWS anomalies, vegetation ET, and soil moisture). These results are also compared with an estimate of the uncertainties of observations (values provided in section *2.8 Calibration/Evaluation Data*), and are discussed in the subsequent sections.

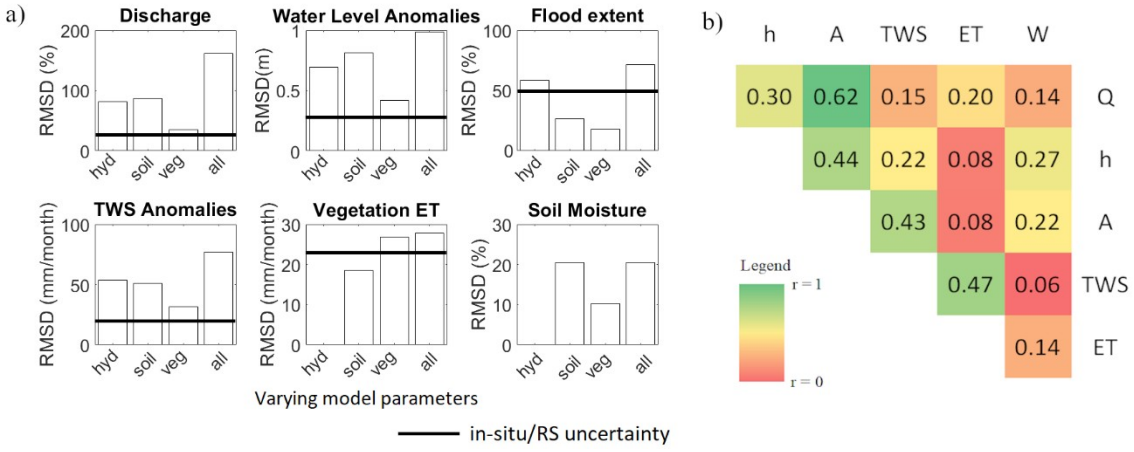

Figure 3. **a)** Sensitivity analysis of different model output variables to varying sets of parameters (hyd=hydraulics, soil, veg=vegetation, and all together). The a priori dispersion of the model parameters, for each output variable, is compared to the reported uncertainty for the in-situ / RS product estimates, previously described in the Cal/Eval data section (no uncertainty estimation is provided for the soil moisture root zone product given absence of this estimate for the Amazon region). **b)** Correlation matrix (Pearson coefficient) between performance metrics (KGE) for the six analyzed variables, by varying all parameters together. KGE values are computed by comparing multiple runs with the reference simulation (i.e., the initial run with the initial parameter set as defined in Supporting Information Table S2). Q = discharge, h = water level, A = flood extent, TWS = total water storage anomalies, ET = vegetation evapotranspiration, W = soil moisture.

3.1.1 How do dispersions in model outputs relate to uncertainties in observations?

Some variables present in-situ/RS observations that have uncertainties significantly lower than the overall dispersion of the model, e.g., 25 % for discharge observations, while model overall parameter dispersion is ~160%. This pattern is also found for water level and TWS estimates, and implies that these observations might be useful to constrain the model. Nonetheless, uncertainties in RS products of flood extent (~50%) and vegetation ET (~23%) are in the same order of magnitude of model overall parameter dispersion, which might hamper their contribution for model calibration, due to their high uncertainties.

44
45
503

504 3.1.2 Which sets of parameters are related to which variables?
505

506 The overall model dispersions are related to different sets of parameters: discharge,
507 water level, and TWS are more strongly related to hydraulics and soil parameters, and to
508 a lesser extent to vegetation parameters. Flood extent estimates are strongly related to
509 hydraulic parameters, and less to soil and vegetation. As expected, soil moisture and
510 vegetation ET estimates relate to vertical water balance processes, being insensitive to
511 hydraulic parameters. Soil moisture (W) is more sensitive to soil parameters, while
512 vegetation ET is more sensitive to vegetation parameters. These results are very useful
513 to understand the RS-based calibration experiments addressed in section 3.2. For
514 instance, if model calibration with ET or W is achieved through optimization of
515 hydraulic parameters, it would highlight that the model would have "gotten the right
516 results for the wrong reasons". The same would occur if flood extent calibration
517 targeted soil or vegetation parameters.

518

519 3.1.3 Which variables are inter-related?
520

521 By varying all parameters together, there is a high correlation (greater or equal to 0.4)
522 between the performance of discharge and flood extent, water level and flood extent,
523 flood extent and TWS, and ET and TWS (Figure 3b). High correlations between
524 discharge, water level and flood extent are expected because of their strong association
525 through river transport processes. However, correlation between discharge and water
526 level is not too high (0.30), and this is probably due to high uncertainties in hydraulic
527 parameters, and to the large distance separating the water level virtual station and the
528 streamflow gauge. Furthermore, high correlations between TWS and flood extent might
529 be related to surface water storage dynamics which are especially relevant in regions
530 with floodplains.

531 In general, a high correlation between variables in Figure 3b should be reflected in
532 positive results when calibrating with a given variable and evaluating with the other
533 highly correlated variable (single-variable calibration). This may also indicate that
534 observations of these variables are redundant if used simultaneously in a multi-
535 calibration framework. However, high correlations in Figure 3b followed by
536 deterioration after the single-variable calibration process might indicate structural errors
537 in the model, or in the observations. We stress however that this study did not attempt to
538 quantify structural errors. Conversely, low correlations in Figure 3b, followed by
539 improvement in performances with the calibration with multiple variables, might
540 indicate complementarity between variables.

541

542 3.2 Model calibration
543

3.2.1 How RS-based model calibration improves discharge estimates?

For the evaluation time period (2006–2008 for discharge, flood extent, TWS, ET and 2013–2014 for water level and soil moisture), calibration with all RS products led to improvements in discharge estimates (Figure 4a). For the calibration time period (2009-2012), TWS, ET and soil moisture RS products also led to improvements in discharge estimates, while water level and flood extent led to discharge overestimation in wet periods (Figure 4a). This could be due to high uncertainties in the observations (Figure 3a), but if this was the case, it would also be reflected in a poor performance for water level and flood extent when discharge is the target variable for calibration (Figure 4b), which does not occur. Therefore, calibration with discharge leads to reasonable parameter sets for the performance of discharge itself, and also water level and flood extent. However, it does not lead to the best hydraulic arrangement, which might be achieved more successfully when calibrating with water level or flood extent.

Nonetheless, both water level and flood extent observations are representative of a specific location in the basin (Figure 2), and calibration with these variables might lead to the best parameter arrangement for these locations, but not for the whole watershed. A more spatially-consistent use of these observations should improve their usability to constrain models and improve discharge estimates, such as the studies of Kittel et al. (2018), that used radar altimetry measurements at 12 locations in the basin, Schneider et al. (2017), that used data from 13 virtual stations, or Liu et al. (2015), that used water level measurements at four virtual stations, and flood extent for stream segments at different locations in the basin.

RS variables as TWS, ET, and soil moisture were able to improve discharge estimates by S =13.7%, S= 52.9%, and S = 27.0% (Figure 5-I, calibration period) or S = 27.4%, S= 6.1%, S= 12.3% (Figure 5-II, evaluation period), which is especially relevant in the context of the Prediction in Ungauged Basins initiative (Hrachowitz et al., 2013; Sivapalan et al., 2003). These results agree with previous studies, such as López et al. (2017) that found good performances in discharge estimates by model calibration with GLEAM ET and ESA CCI soil moisture, or Nijzink et al. (2018), that found improvements in discharge by using soil moisture products (AMSR-E, ASCAT) and TWS from GRACE.

The multi-variable calibration experiment considering all variables except discharge (Figure 5b) resulted in a Skill Score of S = 17.4% for discharge in the evaluation period. This is relevant for estimating discharge in poorly gauged basins. Nonetheless, for the calibration period, Skill Score had a low value (S = 1.7%), reflecting some limitations when retrieving discharges, probably because of potential trade-offs between variables (Koppa et al., 2019). RS uncertainties could be better incorporated into the calibration, for instance by using bias-insensitive metrics (e.g., Demirel et al., 2018; Zink et al., 2018; Dembele et al., 2020), or explicitly including them into the objective functions (Aires, 2014; Croke, 2009; Foglia et al., 2009; Peña-Arancibia et al., 2015).

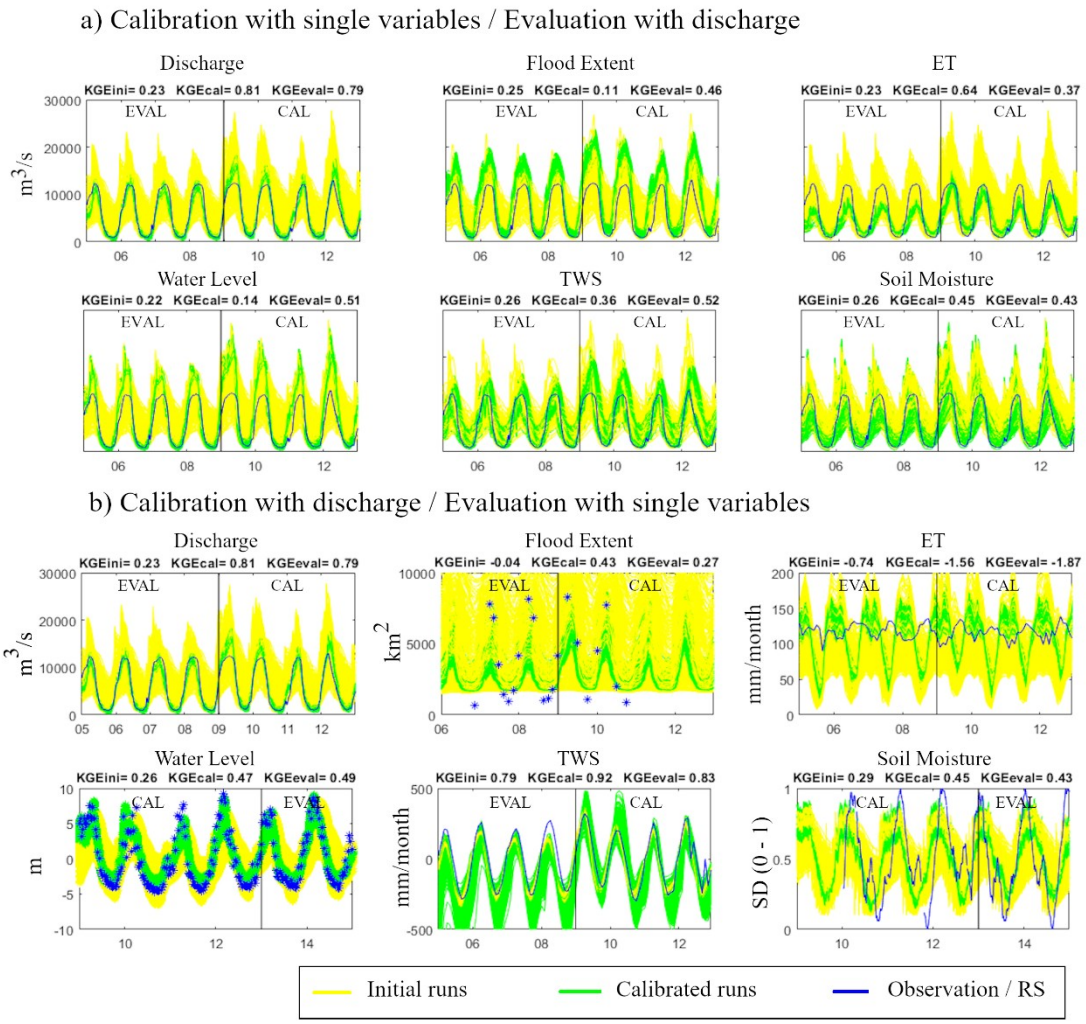

Figure 4. (a) Daily time series of discharge, when calibrating the model with six different variables. (b) Time series of the six variables when calibrating the model with discharge observations only (discharge, water level, flood extent and soil moisture are at a daily time step, while TWS and ET are at a monthly time step). *KGEini* is the mean KGE of initial runs, *KGEcal* is the mean KGE of calibrated runs, evaluated for the same period of calibration, *KGEeval* is the mean KGE of calibrated runs, evaluated for a different period than calibration. Time series for all variables by calibrating the model with all setups is presented in supporting information (Figure S1).

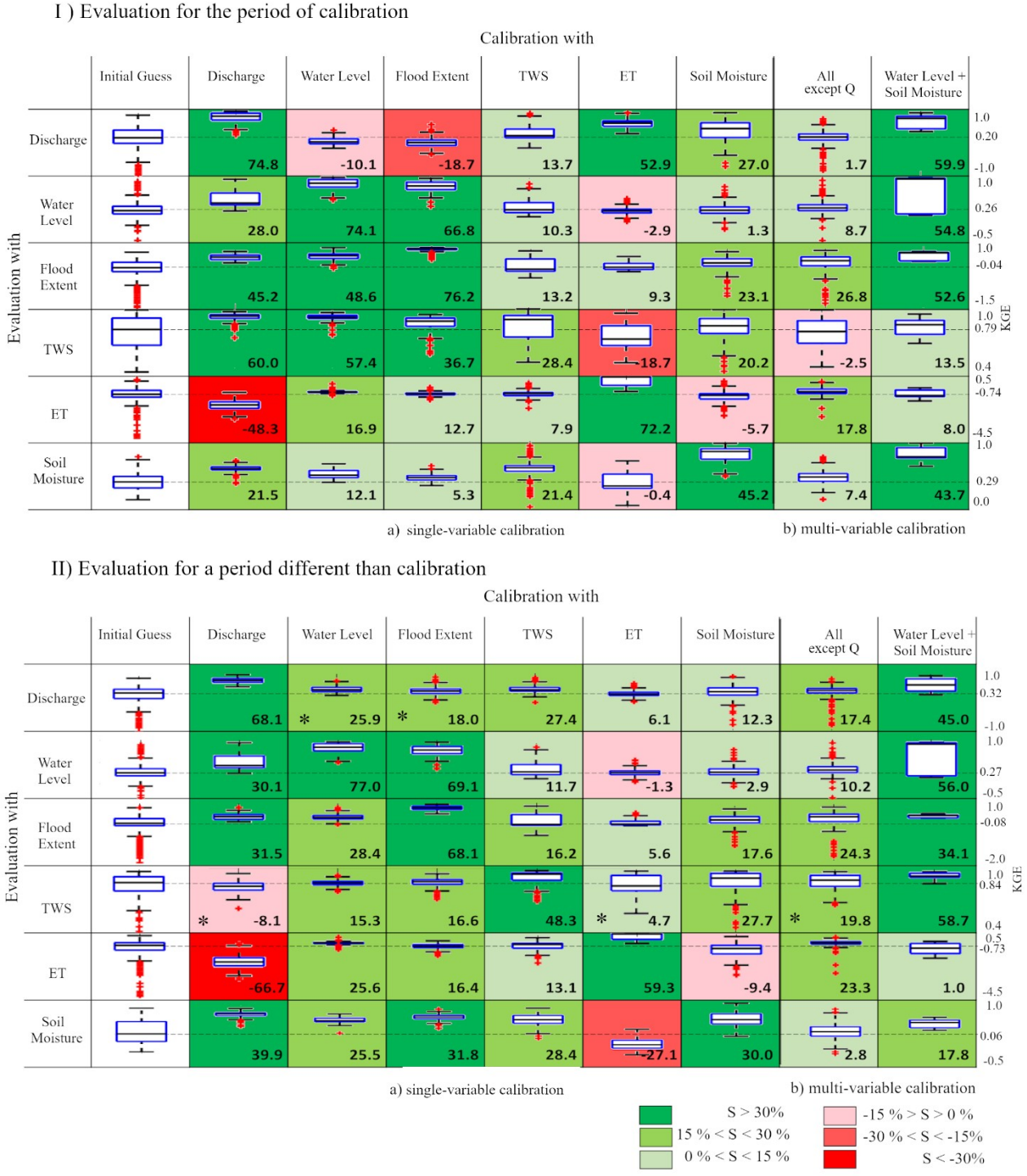

595

596 **Figure 5**. Boxplots of mean KGE for the evaluation of multiple variables with different
597 calibration strategies. (I) Evaluation for the period of calibration (2009 – 2012); (II) Evaluation
598 for a different period than calibration (2006 – 2008 for Q, A, TWS, ET; 2013 – 2014 for h and
599 W). "Initial guess" refers to model runs with the a priori parameter sets. (a) Single-variable
600 (discharge, water level, flood extent, TWS, vegetation ET, soil moisture) and (b) multi-variable
601 calibration (all except discharge, water level + soil moisture). The spread of the values in the
602 boxplots stems from 300 model runs (100 for each of three calibration experiments). Numbers
603 next to the boxplots represent Skill Score (%). Colors refer to classes of skill score. Please note
604 that the KGE scales are different for each variable. Asterisks refer to cases when the evaluation
605 period resulted in a different performance than the calibration period (i.e., positive Skill Score in

calibration followed by negative Skill Score in evaluation, or vice-versa). Please note that Skill Score values are computed based on mean values, while the boxplots depict median values.

3.2.2 How does RS-based model calibration improve the water cycle representation?

When performing a single-variable calibration, the performance of the variable itself always improves, which is evidenced by the positive values in the main diagonal (Figure 5-I-a, for calibration period, and Figure 5-II-a, for evaluation period). Calibration with water level was also able to improve estimates of flood extent, TWS, ET and soil moisture (cal period), and all variables (eval period). Calibration with flood extent improved water level, TWS, ET and soil moisture. Calibration with TWS improved all variables. Calibration with ET was able to improve discharge and flood extent. Calibration with soil moisture improved all variables but ET. Results for calibration and evaluation periods agree (i.e., improvement (positive Skill Score) or deterioration (negative Skill Score) for both cal and eval) in 43 out of the 48 cases (89.6%). In the five remaining cases (10.4%), results between calibration and evaluation periods differ: three of them are in the evaluation with TWS, and two of them are in the discharge evaluation (calibration with water level and flood extent).

In the best modeling scenario, calibration with any variable should improve the performance of all other variables. However, we have identified that this did not happen in our experiments. This can be due to uncertainties in model structure, in parameterization, or in the observations. Previous studies have also found significant advantages in using RS-based model calibration to identify structural model issues (e.g., Werth et al., 2009; Willem Vervoort et al., 2014; Winsemius et al., 2008), detect uncertainties in input data (e.g., Milzow et al., 2011), identify deficiencies in model parameterization (e.g., Franks et al., 1998; Koppa et al., 2019), or increase model reliability (e.g., Koch et al., 2018; Manfreda et al., 2018).

According to Figure 4b and supporting information (Figure S1), calibration with discharge improved estimates of almost all variables. However, calibration with discharge deteriorated the performance for vegetation ET time series. Vegetation ET estimated by MOD16 varies at maximum 30mm/month. MGB calibration with discharge led to ET variations of 100 mm/month, reaching around 30 mm/month in the driest periods, while MOD16 estimates are limited to a minimum of 100 mm/month in these periods (time series in Figure 4b). However, one can notice that not even the seasonality between MGB and MOD16 time series agree. This could be due to relatively high uncertainties in vegetation ET estimates from MOD16 for the Amazon basin (around 23 mm/month, according to Gomis-Cebolla et al., 2019). Nonetheless, it could also be related to model structural and/or parameter deficiencies, in which case the model might be “right for the wrong reasons”. In order to identify the source of this ET inconsistency, we have compared MOD16 and MGB results to in-situ measurements of ET in Purus River Basin, provided by Gomis-Cebolla et al. (2019) and Maeda et al. (2017). We found a much stronger agreement both in seasonality and in amplitude of in-situ observations with MOD16 observations than with MGB model output. Hasler &

650 Avissar (2007) and Pan et al (2020) have already warned about the overestimation of
651 dry season water stress in hydrological models, probably related to the
652 misrepresentation of soil water availability for plants. This was also found by Maeda et
653 al. (2017), which highlighted that ET was not water-limited because of the plants'
654 access to deep soil water, which has also been previously documented by Nepstad et al.
655 (1994). They found that, in the Southern Amazon ecotone, deep root water intake plays
656 a key role in maintaining ecosystem productivity during dry season. MGB model is
657 probably misrepresenting these processes, which would remain unknown if it were only
658 compared to discharge time series.

659 Even though the calibration with discharge observations was not able to accurately
660 estimate ET, calibration with the remaining variables (except for soil moisture) was able
661 to improve ET estimates. For instance, in Figure 3b, ET and water level presented low
662 correlation (r = 0.08), but calibration with water level improved ET estimates by S =
663 16.9% (cal period) and S = 25.6% (eval period). However, in Figure 3b, ET and TWS
664 presented high correlation (r=0.47), but calibration with TWS improved ET estimates
665 by only S = 7.9% (cal period) and S = 13.1% (eval period).

666 In general, calibration with TWS did not present much influence on any of the variables.
667 In spite of some improvements, skill scores were usually low. Consistently, TWS
668 estimates got relatively easily improved by calibration with any variable (except for ET,
669 for cal period; or discharge, for eval period). These results for TWS contrast with
670 previous work from Lo et al. (2010), Nijzink et al. (2018), Rakovec et al. (2016),
671 Schumacher et al. (2018), and Werth & Güntner (2010), which highlighted the value of
672 GRACE data when incorporated into hydrological modeling. This can be due to the
673 high seasonality of Purus River Basin, in which TWS does not aggregate much
674 information, biasing the calibration with high correlation values. Even for the initial
675 guess (uncalibrated) setup TWS performances were already very good: KGE values
676 were around 0.8, while for all other variables, except for ET (for which KGE values
677 were negative), KGE values were around 0.3 for the uncalibrated setup.

678 Flood extent and water level performances were improved by calibration with
679 discharge, water level and flood extent, but it did not affect much ET (which actually
680 was degraded with discharge calibration) and soil moisture. This is probably due to the
681 relationship between water level and flood extent with river transport processes (e.g.,
682 flood routing and floodplain storage), while ET and soil moisture are more related to
683 vertical hydrological processes (e.g., soil water balance). This highlights the
684 complementarity between variables that relate to different processes.

685 Calibration with soil moisture improves performances of all variables (water level to a
686 lesser extent), except for ET. Consistently, calibration with all variables (except ET) are
687 able to improve soil moisture to some extent.

688

689 **3.2.3 What is the added value of complementary RS observations?**
690

691 By calibrating with all variables together except Q (Figure 5b), we found improvements
692 for almost all variables, with the most significant improvements for flood extent (S =
693 25% for cal and eval periods) and ET (S = 20% for cal and eval periods). For discharge,
694 performance for the evaluation period was improved (S = 17.4%), which is important
695 for estimating discharge in poorly gauged basins. However, for the calibration period,
696 Skill Score for discharge performance was S = 1.7%, which might reflect some
697 limitations in retrieving discharge based on the calibration of the RS-derived variables,
698 as discussed previously.

699 Therefore, we chose a specific arrangement of two complementary variables in order to
700 check if this calibration setup might lead to better retrievals for discharge and the other
701 variables. The chosen variables were soil moisture and water level, because of their
702 complementarity. Based on the Skill Score values in Figure 5-I, calibration with water
703 level only improves all variables but discharge (and soil moisture to a lesser extent),
704 while calibration with soil moisture only improves all variables, but ET (and water level
705 to a lesser extent).

706 The calibration arrangement of water level and soil moisture led to improvements not
707 only to soil moisture and water level themselves, but also to all other variables (ET to a
708 lesser extent). For instance, flood extent was improved by S = 52.6% and S = 34.1%
709 (cal and eval period, respectively). Discharge was improved by S = 59.9%, with a
710 resulting mean KGE = 0.70 for the calibration period (S = 45.0% and mean KGE = 0.35
711 for evaluation period). These results agree with previous works that found an
712 improvement in model performances by multi-variable calibration of soil moisture and
713 evapotranspiration (e.g., Koppa et al., 2019; López et al., 2017), discharge and
714 evapotranspiration (e.g., Herman et al., 2018; Pan et al., 2018; Poméon et al., 2018),
715 discharge and soil moisture (e.g., Li et al., 2018; Rajib et al., 2016), discharge and TWS
716 (e.g., Rakovec et al., 2016; Schumacher et al., 2018; Werth & Güntner, 2010), and
717 discharge and water level (e.g., Kittel et al., 2018; Schneider et al., 2017; W. Sun et al.,
718 2012). However, it is difficult to compare this study to previous works, because most of
719 them used discharge observations as constraints. In this study, we avoided the use of
720 discharge observations for multi-variable calibration, in order to analyze the
721 applicability of the RS-based calibration method for poorly-gauged regions.

722 Calibration with water level and soil moisture did not present much influence on ET
723 performance, because of the specificities regarding ET in this watershed, i.e., given that
724 the model setup does not represent deep root water intake during dry season, as
725 discussed previously.

726 By comparing the two frameworks for multi-variable calibration (all except Q versus
727 h+W calibration), we found that calibration with all variables except Q is useful to some
728 extent, but consistently selecting complementary variables for model calibration
729 resulted in best overall performance.

730

731 **3.3 Are we getting the right results for the right sets of parameters?**
732

733 When analyzing the dispersions of parameters before and after calibration with each
734 variable (Figure 6 for a few selected parameters, Supporting Information Figure S2 for
735 all calibrated parameters), it can be observed that the range of parameters vary largely
736 depending on the calibration variable. For instance, Wm is a soil conceptual parameter
737 related to maximum water storage in the soil. In the calibration based on single
738 variables (except ET) it converged to low values (300 mm), while in the calibration with
739 ET it reached high values (2000 mm). This probably occurred in order to compensate,
740 by overparameterization, a structural error in the model, i.e., the model inability to
741 represent deep root water uptake in dry season. These trade-offs between model
742 parameters during calibration has also been reported and discussed by Koppa et al.
743 (2019).

744 The surface resistance parameter also resulted in a wide range of values depending on
745 the calibration target variable. When calibrated with water level, flood extent, or 'all
746 except Q' experiments, it reached median values higher than 150 s/m, but calibration
747 with h+W led to median values lower than 50 s/m. Surface resistance is a vegetation
748 parameter directly related to ET dynamics, so it is important to note that calibration with
749 ET was able to reduce the dispersion of this parameter, reaching a median value of
750 about 80 s/m (similar to calibration with Q and W).

751 Another interesting result relates to channel Manning's coefficient, which presented
752 different values for each calibration experiment. This agrees with previous findings
753 about Manning parameter being often used as an effective parameter that compensates
754 for neglected hydrodynamic processes as localized channel head losses, poor cross
755 section representation, or non-represented 2D processes (Neal et al 2015).

756 Many previous studies have highlighted the use of multi-variable calibration to narrow
757 parameters' search space (Nijzink et al., 2018; W. Sun et al., 2018), but this was not
758 observed in our results. Based on the limited multi-variable calibration experiments
759 performed here ('all except Q' and h+W), no narrowing in parameters' search space
760 was found. For most parameters (except for Wm), calibration with 'all except Q' and
761 h+W resulted in a wide range of values. This can be due to differing convergence sets of
762 parameters between each of the triplicate runs. A more robust experiment comparing
763 more multi-variable calibration strategies (e.g., Q + different R-based variables) might
764 provide better understanding on this topic.

765

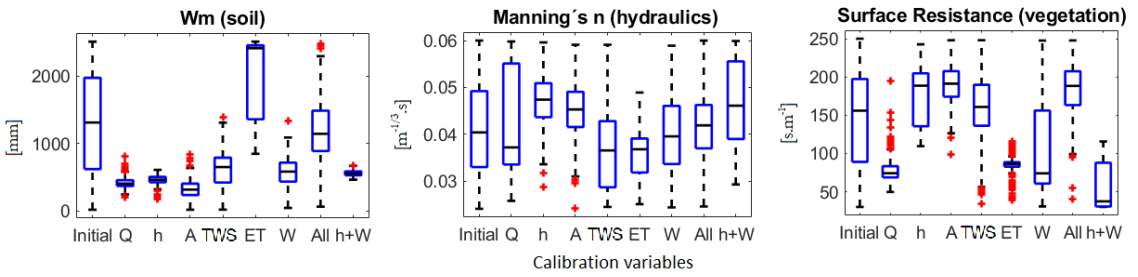

766

767 **Figure 6**. Boxplots of dispersion of three model parameters before (Initial) and after the single-
768 variable calibration (Q – discharge; h – water level; A – flood extent; TWS – total water
769 storage anomalies; ET - vegetation ET; W – soil moisture), and multi-variable calibration (All

68
69
770 – variables except discharge; h+W – water level and soil moisture). The spread of the values in
771 the boxplots stems from 300 model runs (100 for each calibration experiment). Description of
772 parameters is presented in Supporting Information Table S2. A complete figure with boxplots
773 for all parameters is presented in Supporting Information Figure S2.

774

775 **3.4 Spatial Evaluation**
776

777 For model calibration, we used one streamflow gauge for discharge, one virtual station
778 for water level, and averaged RS data for the whole basin for TWS, ET and soil
779 moisture. However, many recent studies investigated the potential for using RS spatially
780 distributed information in model calibration, for instance with bias-insensitive metrics
781 (Demirel et al., 2018; Zink et al., 2018; Dembele et al., 2020). Here we further analyze
782 how the lumped calibration affected the simulated spatial patterns (Figure 7; Figure S3
783 in Supporting Information).

784 For discharge, water level, flood extent and TWS, spatial patterns are well reproduced
785 even when running the model with the initial parameter set, because the spatial patterns
786 of these variables are determined by intrinsic characteristics of the basin. Nonetheless,
787 for ET, the spatial patterns are completely different between the initial parameter set and
788 the calibrated setup. In this case, the calibration with spatially aggregated ET was able
789 to recover the spatial representation of MOD16. A similar result was found for soil
790 moisture spatial representation by Demirel et al. (2019), that calibrated a model with
791 spatially aggregated soil moisture and TWS data.

792 In summary, these results highlight the overall model capability to retrieve the ET
793 spatial pattern even by using a lumped calibration approach. However, for other
794 variables, the spatial pattern was not considerably affected by the differing model
795 calibration strategies.

796

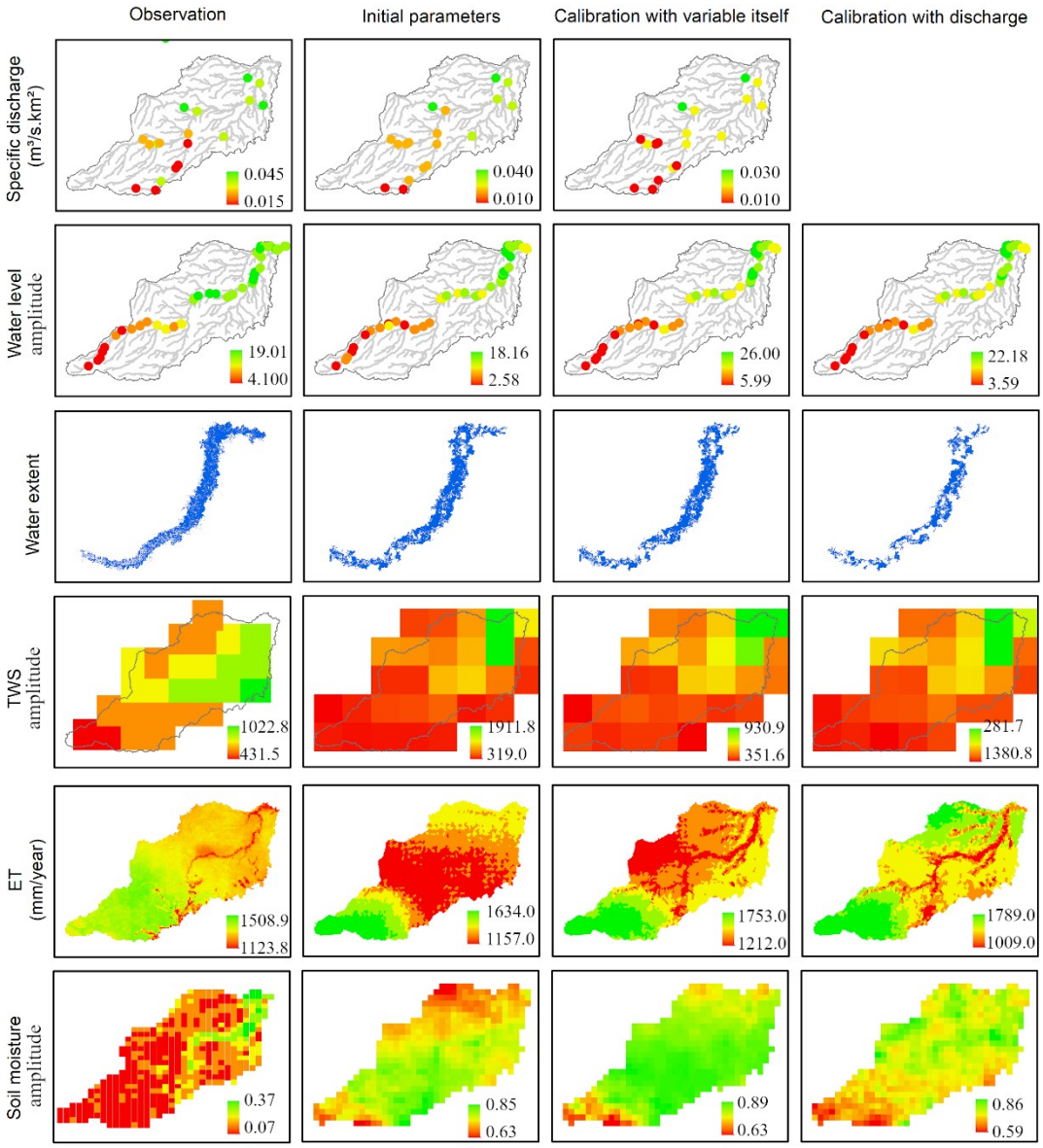

Figure 7. Spatial distribution of variables. Columns: RS observation, model run with the initial parameter set, model run with the best parameter set (calibrated for each variable), model run with the best parameter set (when calibrated with discharge). Complete figure is presented in Figure S3 (Supporting Information).

4 Conclusion

We calibrated and evaluated a hydrological-hydrodynamic model with five different RS-based observations of the water cycle: water levels (Jason-2), flood extent (ALOS-PALSAR), TWS (GRACE), vegetation ET (MOD16), and soil moisture (SMOS), for a study basin in a tropical region with floodplains (Purus River Basin in the Amazon), and analyzed the redundancy and complementarity between different variables and processes.

Results showed that calibration with current RS observations was able to improve discharge estimates. For instance, in the uncalibrated setup (a priori parameter sets), average performances for discharge were around KGE = 0.30. By calibrating the model with ET from MOD16 (and evaluating for the same time period), discharge average performance was improved to KGE = 0.64, representing a Skill Score of S = 52.9%. Also in the calibration period, a joint scheme of calibration with water level + soil moisture led to discharge improvements of S = 59.9%. When evaluating for a different time period, discharge performance was improved by calibration with water level, TWS and a joint scheme of all RS-variables (S = 25.9%, S = 27.9% and S = 17.4%, respectively). We conclude that RS observations are useful to predict discharge estimates. However, the utility of each RS variable might depend on the study area characteristics and the time period considered.

Our results also showed that RS-based calibration led to an overall improvement of the water cycle representation. For instance, calibration with water level was able to improve estimates of water level itself, but also flood extent, TWS and ET; calibration with soil moisture was able to improve estimates of soil moisture itself, but also discharge, flood extent and TWS.

Moreover, calibration with multiple RS variables was able to highlight deficiencies that might be related to model structure, parameterization, and observations. In the context of model structure, for instance, calibration with ET highlighted the model inability to represent the root water intake in dry season in this region, thus compensating it by misrepresenting other variables. In the context of model parameterization, for instance, we found a wide range of different parameters by varying the calibration target variable.

Besides individual calibration with each RS variable, we conducted two multi-variable calibration experiments: calibration with all variables except discharge, and calibration with water level and soil moisture. Calibration with all variables was useful to some extent, but appropriately selecting complementary variables for model calibration may result in a better overall performance. Even though we used a lumped calibration approach, results highlighted the overall model capability to retrieve ET spatial pattern, but not for TWS and soil moisture.

The main conclusions presented here are of great interest for the hydrological community, and agree with previous works in that RS–based calibration is useful to improve the water cycle representation in hydrological models. To further investigate the potentiality of RS data, future developments should test the methodology presented here for multiple basins at contrasting hydro-climatic regions. Here, we assessed an Amazonian Equatorial basin, with particular climate and land cover characteristics and an overall spatial homogeneity of rainfall-runoff processes. Other basins with different hydroclimatic regimes could be also assessed, e.g., in arid basins subject to long dry periods, more erratic precipitation patterns, and different runoff generation mechanisms than the Amazon, which require different model structures.

Finally, here we used one state-of-the-art RS product for each variable, but future developments should explore to its potential other missions as SWOT for surface water observation (Biancamaria et al., 2016), as well as considering different products for

853 representing each variable (e.g., ET could be estimated by GLEAM, MODIS, SSEBop,
854 SEBS, ALEXI, METRIC, etc., besides MOD16).

855

856 **Acknowledgements**

857 This study was financed in part by the Coordenação de Aperfeiçoamento de Pessoal de
858 Nível Superior - Brasil (CAPES) - Finance Code 001, and the Conselho Nacional de
859 Desenvolvimento Científico e Tecnológico (CNPq) – Grant Number 41161/2017-5. It
860 was conducted in the context of the SWOT-MOD science team project from SWOT
861 satellite mission. We would also like to thank colleagues from the Large Scale
862 Hydrology Group (HGE/IPH) for general discussions about this study. Data presented
863 in this study are available at <https://doi.org/10.5281/zenodo.3956609> (MGB code in
864 FORTRAN, MGB Input folder, post-processing code in MATLAB).

865

866 **References**

867 Aires, F. (2014). Combining Datasets of Satellite-Retrieved Products. Part I:
868 Methodology and Water Budget Closure. *Journal of Hydrometeorology*.
869 https://doi.org/10.1175/jhm-d-13-0148.1

870 Alkama, R., Decharme, B., Douville, H., Becker, M., Cazenave, A., Sheffield, J., et al.
871 (2010). Global evaluation of the ISBA-TRIP continental hydrological system. Part
872 I: Comparison to GRACE terrestrial water storage estimates and in situ river
873 discharges. *Journal of Hydrometeorology*. https://doi.org/10.1175/2010JHM1211.1

874 Asadzadeh Jarihani, A., Callow, J. N., Johansen, K., & Gouweleeuw, B. (2013).
875 Evaluation of multiple satellite altimetry data for studying inland water bodies and
876 river floods. *Journal of Hydrology*. https://doi.org/10.1016/j.jhydrol.2013.09.010

877 Di Baldassarre, G., & Montanari, A. (2009). Uncertainty in river discharge
878 observations: A quantitative analysis. *Hydrology and Earth System Sciences*.
879 https://doi.org/10.5194/hess-13-913-2009

880 Baroni, G., Schalge, B., Rakovec, O., Kumar, R., Schüler, L., Samaniego, L., et al.
881 (2019). A Comprehensive Distributed Hydrological Modeling Intercomparison to
882 Support Process Representation and Data Collection Strategies. *Water Resources
883 Research*. https://doi.org/10.1029/2018WR023941

884 Bates, P. D., Horritt, M. S., & Fewtrell, T. J. (2010). A simple inertial formulation of
885 the shallow water equations for efficient two-dimensional flood inundation
886 modelling. *Journal of Hydrology*. https://doi.org/10.1016/j.jhydrol.2010.03.027

887 Beven, K. (2006). A manifesto for the equifinality thesis. In *Journal of Hydrology*.
888 https://doi.org/10.1016/j.jhydrol.2005.07.007

889 Beven, K., & Binley, A. (1992). The future of distributed models: Model calibration and
890 uncertainty prediction. *Hydrological Processes*.
891 https://doi.org/10.1002/hyp.3360060305

892 Blöschl, G., Bierkens, M. F. P., Chambel, A., Cudennec, C., Destouni, G., Fiori, A., et
893 al. (2019). Twenty-three Unsolved Problems in Hydrology (UPH)—A community

894 perspective. *Hydrological Sciences Journal.*
895 https://doi.org/10.1080/02626667.2019.1620507

896 Brêda, J. P. L. F., Paiva, R. C. D., Bravo, J. M., Passaia, O. A., & Moreira, D. M.
897 (2019). Assimilation of Satellite Altimetry Data for Effective River Bathymetry.
898 *Water Resources Research*. https://doi.org/10.1029/2018wr024010

899 Clark, M. P., Fan, Y., Lawrence, D. M., Adam, J. C., Bolster, D., Gochis, D. J., et al.
900 (2015). Improving the representation of hydrologic processes in Earth System
901 Models. *Water Resources Research*. https://doi.org/10.1002/2015WR017096

902 Collischonn, B., Collischonn, W., & Tucci, C. E. M. (2008). Daily hydrological
903 modeling in the Amazon basin using TRMM rainfall estimates. *Journal of*
904 *Hydrology*. https://doi.org/10.1016/j.jhydrol.2008.07.032

905 Collischonn, W., Allasia, D., da Silva, B. C., & Tucci, C. E. M. (2007). The MGB-IPH
906 model for large-scale rainfall-runoff modelling. *Hydrological Sciences Journal*.
907 https://doi.org/10.1623/hysj.52.5.878

908 Croke, B. F. W. (2009). Representing uncertainty in objective functions: Extension to
909 include the influence of serial correlation. In *18th World IMACS Congress and*
910 *MODSIM09 International Congress on Modelling and Simulation: Interfacing*
911 *Modelling and Simulation with Mathematical and Computational Sciences,*
912 *Proceedings*.

913 Crow, W. T., Wood, E. F., & Pan, M. (2003). Multiobjective calibration of land surface
914 model evapotranspiration predictions using streamflow observations and
915 spaceborne surface radiometric temperature retrievals. *Journal of Geophysical*
916 *Research D: Atmospheres*. https://doi.org/10.1029/2002JD003292

917 Demirel, M. C., Mai, J., Mendiguren, G., Koch, J., Samaniego, L., & Stisen, S. (2018).
918 Combining satellite data and appropriate objective functions for improved spatial
919 pattern performance of a distributed hydrologic model. *Hydrology and Earth*
920 *System Sciences.* https://doi.org/10.5194/hess-22-1299-2018

921 Demirel, M. C., Özen, A., Orta, S., Toker, E., Demir, H. K., Ekmekcioglu, Ö., Taysi,
922 H., Eruçar, S., Sag, A. B., Sari, Ö., Tuncer, E., Hanci, H., Özcan, T. I., Erdem, H.,
923 Kosucu, M. M., Basakin, E. E., Ahmed, K., Anwar, A., Avcuoglu, M. B., Vanli,
924 Ö., Stisen, S., & Booij, M. J. (2019). Additional value of using satellite-based soil
925 moisture and two sources of groundwater data for hydrological model calibration.
926 *Water.* https://doi.org/10.3390/w11102083

927 Duan, Q., Sorooshian, S., & Gupta, V. (1992). Effective and efficient global
928 optimization for conceptual rainfall−runoff models. *Water Resources Research*.
929 https://doi.org/10.1029/91WR02985

930 Fan, F. M., Buarque, D. C., Pontes, P. R. M., & Collischonn, W. (2015). Um mapa de
931 Unidades de Resposta Hidrológica para a América do Sul. *XXI Simpósio Brasileiro*
932 *de Recursos Hídricos*.

933 Fleischmann, A.S., Paiva, R.C.D., Collischonn, W., Siqueira, V.A., Paris, A., Moreira,
934 D.M., Papa, F., Bitar, A.A., Parrens, M., Aires, F. & Garambois, P.A. (2020).
935 Trade−offs between 1D and 2D regional river hydrodynamic models. *Water*
936 *Resources Research.* https://doi.org/10.1029/2019WR026812

937 Foglia, L., Hill, M. C., Mehl, S. W., & Burlando, P. (2009). Sensitivity analysis,
938 calibration, and testing of a distributed hydrological model using error-based
939 weighting and one objective function. *Water Resources Research*.
940 https://doi.org/10.1029/2008WR007255

941 Franks, S. W., Gineste, P., Beven, K. J., & Merot, P. (1998). On constraining the
942 predictions of a distributed model: The incorporation of fuzzy estimates of
943 saturated areas into the calibration process. *Water Resources Research*.
944 https://doi.org/10.1029/97WR03041

945 Gharari, S., Shafiei, M., Hrachowitz, M., Kumar, R., Fenicia, F., Gupta, H. V., &
946 Savenije, H. H. G. (2014). A constraint-based search algorithm for parameter
947 identification of environmental models. *Hydrology and Earth System Sciences*.
948 https://doi.org/10.5194/hess-18-4861-2014

949 Gomis-Cebolla, J., Jimenez, J. C., Sobrino, J. A., Corbari, C., & Mancini, M. (2019).
950 Intercomparison of remote-sensing based evapotranspiration algorithms over
951 amazonian forests. *International Journal of Applied Earth Observation and*
952 *Geoinformation*. https://doi.org/10.1016/j.jag.2019.04.009

953 Grimaldi, S., Schumann, G. J. P., Shokri, A., Walker, J. P., & Pauwels, V. R. N. (2019).
954 Challenges, Opportunities, and Pitfalls for Global Coupled Hydrologic-Hydraulic
955 Modeling of Floods. *Water Resources Research*.
956 https://doi.org/10.1029/2018WR024289

957 Gupta, H. V., Kling, H., Yilmaz, K. K., & Martinez, G. F. (2009). Decomposition of the
958 mean squared error and NSE performance criteria: Implications for improving
959 hydrological modelling. *Journal of Hydrology*.
960 https://doi.org/10.1016/j.jhydrol.2009.08.003

961 Haddeland, I., Skaugen, T., & Lettenmaier, D. P. (2006). Anthropogenic impacts on
962 continental surface water fluxes. *Geophysical Research Letters*.
963 https://doi.org/10.1029/2006GL026047

964 Hasler, N., & Avissar, R. (2007). What controls evapotranspiration in the Amazon
965 basin? *Journal of Hydrometeorology*. https://doi.org/10.1175/JHM587.1

966 Herman, M. R., Nejadhashemi, A. P., Abouali, M., Hernandez-suarez, S., Daneshvar,
967 F., Zhang, Z., et al. (2017). Evaluating the Role of Evapotranspiration Remote
968 Sensing Data in Improving Hydrological Modeling Predictability. *Journal of*
969 *Hydrology*. https://doi.org/10.1016/j.jhydrol.2017.11.009

970 Hess, L. L., Melack, J. M., Novo, E. M. L. M., Barbosa, C. C. F., & Gastil, M. (2003).
971 Dual-season mapping of wetland inundation and vegetation for the central Amazon
972 basin. *Remote Sensing of Environment*. https://doi.org/10.1016/j.rse.2003.04.001

973 Hodges, B. R. (2013). Challenges in continental river dynamics. *Environmental*
974 *Modelling and Software*. https://doi.org/10.1016/j.envsoft.2013.08.010

975 Holeman, J. N. (1968). The Sediment Yield of Major Rivers of the World. *Water*
976 *Resources Research*. https://doi.org/10.1029/WR004i004p00737

977 Houser, P. R., Shuttleworth, W. J., Famiglietti, J. S., Gupta, H. V., Syed, K. H., &
978 Goodrich, D. C. (1998). Integration of soil moisture remote sensing and hydrologic
979 modeling using data assimilation. *Water Resources Research*.

980 https://doi.org/10.1029/1998WR900001

981 Hrachowitz, M., Savenije, H. H. G., Blöschl, G., McDonnell, J. J., Sivapalan, M.,
982 Pomeroy, J. W., et al. (2013). A decade of Predictions in Ungauged Basins (PUB)-
983 a review. *Hydrological Sciences Journal*.
984 https://doi.org/10.1080/02626667.2013.803183

985 Huffman, G. J., Adler, R. F., Bolvin, D. T., Gu, G., Nelkin, E. J., Bowman, K. P., et al.
986 (2007). The TRMM Multisatellite Precipitation Analysis (TMPA): Quasi-global,
987 multiyear, combined-sensor precipitation estimates at fine scales. *Journal of*
988 *Hydrometeorology*. https://doi.org/10.1175/JHM560.1Jiang, D., & Wang, K.
989 (2019). The Role of Satellite-Based Remote Sensing in Improving Simulated
990 Streamflow: A Review. *Water*. https://doi.org/10.3390/w11081615

991 Junk, W. J. (1997). General Aspects of Floodplain Ecology with Special Reference to
992 Amazonian Floodplains. https://doi.org/10.1007/978-3-662-03416-3_1

993 Karthikeyan, L., Pan, M., Wanders, N., Kumar, D. N., & Wood, E. F. (2017). Four
994 decades of microwave satellite soil moisture observations: Part 2. Product
995 validation and inter-satellite comparisons. *Advances in Water Resources*.
996 https://doi.org/10.1016/j.advwatres.2017.09.010

997 Kerr, Y. H., Waldteufel, P., Wigneron, J. P., Martinuzzi, J. M., Font, J., & Berger, M.
998 (2001). Soil moisture retrieval from space: The Soil Moisture and Ocean Salinity
999 (SMOS) mission. *IEEE Transactions on Geoscience and Remote Sensing*.
1000 https://doi.org/10.1109/36.942551

1001 Kirchner, J. W. (2006). Getting the right answers for the right reasons: Linking
1002 measurements, analyses, and models to advance the science of hydrology. *Water*
1003 *Resources Research*. https://doi.org/10.1029/2005WR004362

1004 Kittel, C., Nielsen, K., Tøttrup, C., & Bauer-Gottwein, P. (2018). Informing a
1005 hydrological model of the Ogooué with multi-mission remote sensing data.
1006 *Hydrology and Earth System Sciences*. https://doi.org/10.5194/hess-22-1453-2018

1007 Koch, J., Demirel, M. C., & Stisen, S. (2018). The SPAtial EFficiency metric (SPAEF):
1008 Multiple-component evaluation of spatial patterns for optimization of hydrological
1009 models. *Geoscientific Model Development*. https://doi.org/10.5194/gmd-11-1873-
1010 2018

1011 Koppa, A., Gebremichael, M., & Yeh, W. W. G. (2019). Multivariate calibration of
1012 large scale hydrologic models: The necessity and value of a Pareto optimal
1013 approach. *Advances in Water Resources*.
1014 https://doi.org/10.1016/j.advwatres.2019.06.005

1015 Kottek, M., Grieser, J., Beck, C., Rudolf, B., & Rubel, F. (2006). World map of the
1016 Köppen-Geiger climate classification updated. *Meteorologische Zeitschrift*. https://
1017 doi.org/10.1127/0941-2948/2006/0130

1018 Lambin, J., Morrow, R., Fu, L. L., Willis, J. K., Bonekamp, H., Lillibridge, J., et al.
1019 (2010). The OSTM/Jason-2 Mission. *Marine Geodesy*.
1020 https://doi.org/10.1080/01490419.2010.491030

1021 Lee, H., Jung, H. C., Yuan, T., Beighley, R. E., & Duan, J. (2014). Controls of
1022 Terrestrial Water Storage Changes Over the Central Congo Basin Determined by

1023 Integrating PALSAR ScanSAR, Envisat Altimetry, and GRACE Data. In *Remote*
1024 *Sensing of the Terrestrial Water Cycle*.
1025 https://doi.org/10.1002/9781118872086.ch7

1026 Lettenmaier, D. P., Alsdorf, D., Dozier, J., Huffman, G. J., Pan, M., & Wood, E. F.
1027 (2015). Inroads of remote sensing into hydrologic science during the WRR era.
1028 *Water Resources Research*. https://doi.org/10.1002/2015WR017616

1029 Li, Y., Grimaldi, S., Pauwels, V. R. N., & Walker, J. P. (2018). Hydrologic model
1030 calibration using remotely sensed soil moisture and discharge measurements: The
1031 impact on predictions at gauged and ungauged locations. *Journal of Hydrology*.
1032 https://doi.org/10.1016/j.jhydrol.2018.01.013

1033 Liang, X., Lettenmaier, D. P., Wood, E. F., & Burges, S. J. (1994). A simple
1034 hydrologically based model of land surface water and energy fluxes for general
1035 circulation models. *Journal of Geophysical Research*.
1036 https://doi.org/10.1029/94jd00483

1037 Lo, M. H., Famiglietti, J. S., Yeh, P. J. F., & Syed, T. H. (2010). Improving parameter
1038 estimation and water table depth simulation in a land surface model using GRACE
1039 water storage and estimated base flow data. *Water Resources Research*.
1040 https://doi.org/10.1029/2009WR007855

1041 López, P. L., Sutanudjaja, E. H., Schellekens, J., Sterk, G., & Bierkens, M. F. P. (2017).
1042 Calibration of a large-scale hydrological model using satellite-based soil moisture
1043 and evapotranspiration products. *Hydrology and Earth System Sciences*.
1044 https://doi.org/10.5194/hess-21-3125-2017

1045 Maeda, E. E., Ma, X., Wagner, F. H., Kim, H., Oki, T., Eamus, D., & Huete, A. (2017).
1046 Evapotranspiration seasonality across the Amazon Basin. *Earth System Dynamics*.
1047 https://doi.org/10.5194/esd-8-439-2017

1048 Manfreda, S., Mita, L., Dal Sasso, S. F., Samela, C., & Mancusi, L. (2018). Exploiting
1049 the use of physical information for the calibration of a lumped hydrological model.
1050 *Hydrological Processes*. https://doi.org/10.1002/hyp.11501

1051 Maurer, E. P., Adam, J. C., & Wood, A. W. (2009). Climate model based consensus on
1052 the hydrologic impacts of climate change to the Rio Lempa basin of Central
1053 America. *Hydrology and Earth System Sciences*. https://doi.org/10.5194/hess-13-
1054 183-2009

1055 Milzow, C., Krogh, P. E., & Bauer-Gottwein, P. (2011). Combining satellite radar
1056 altimetry, SAR surface soil moisture and GRACE total storage changes for
1057 hydrological model calibration in a large poorly gauged catchment. *Hydrology and*
1058 *Earth System Sciences*. https://doi.org/10.5194/hess-15-1729-2011

1059 Mitchell, K. E., Lohmann, D., Houser, P. R., Wood, E. F., Schaake, J. C., Robock, A.,
1060 et al. (2004). The multi-institution North American Land Data Assimilation
1061 System (NLDAS): Utilizing multiple GCIP products and partners in a continental
1062 distributed hydrological modeling system. *Journal of Geophysical Research D:*
1063 *Atmospheres*. https://doi.org/10.1029/2003JD003823

1064 Montanari, A., & Koutsoyiannis, D. (2014). Modeling and mitigating natural hazards:
1065 Stationarity is immortal! *Water Resources Research*.
1066 https://doi.org/10.1002/2014WR016092

1067 Motovilov, Y. G., Gottschalk, L., Engeland, K., & Rodhe, A. (1999). Validation of a
1068 distributed hydrological model against spatial observations. *Agricultural and*
1069 *Forest Meteorology*. https://doi.org/10.1016/S0168-1923(99)00102-1

1070 Mu, Q., Zhao, M., & Running, S. W. (2011). Improvements to a MODIS global
1071 terrestrial evapotranspiration algorithm. *Remote Sensing of Environment*.
1072 https://doi.org/10.1016/j.rse.2011.02.019

1073 Naz, B. S., Frans, C. D., Clarke, G. K. C., Burns, P., & Lettenmaier, D. P. (2014).
1074 Modeling the effect of glacier recession on streamflow response using a coupled
1075 glacio-hydrological model. *Hydrology and Earth System Sciences*.
1076 https://doi.org/10.5194/hess-18-787-2014

1077 Neal, J.C., Odoni, N. A., Trigg, M.A., Freer, J. E., Garcia-Pintado, J., & Mason, D. C.
1078 (2015). Efficient incorporation of channel cross-section geometry uncertainty into
1079 regional and global scale flood inundation models. *Journal of Hydrology*.
1080 https://doi.org/10.1016/j.jhydrol.2015.07.026

1081 Neal, J., Schumann, G., & Bates, P. (2012). A subgrid channel model for simulating
1082 river hydraulics and floodplain inundation over large and data sparse areas. *Water*
1083 *Resources Research*. https://doi.org/10.1029/2012WR012514

1084 Nearing, G. S., Tian, Y., Gupta, H. V., Clark, M. P., Harrison, K. W., & Weijs, S. V.
1085 (2016). A philosophical basis for hydrological uncertainty. *Hydrological Sciences*
1086 *Journal*. https://doi.org/10.1080/02626667.2016.1183009

1087 Nepstad, D. C., De Carvalho, C. R., Davidson, E. A., Jipp, P. H., Lefebvre, P. A.,
1088 Negreiros, G. H., et al. (1994). The role of deep roots in the hydrological and
1089 carbon cycles of Amazonian forests and pastures. *Nature*.
1090 https://doi.org/10.1038/372666a0

1091 New, M., Hulme, M., & Jones, P. (2000). Representing twentieth-century space-time
1092 climate variability. Part II: Development of 1901-96 monthly grids of terrestrial
1093 surface climate. *Journal of Climate*. https://doi.org/10.1175/1520-
1094 0442(2000)013<2217:RTCSTC>2.0.CO;2

1095 Nijzink, R. C., Almeida, S., Pechlivanidis, I. G., Capell, R., Gustafssons, D., Arheimer,
1096 B., et al. (2018). Constraining Conceptual Hydrological Models With Multiple
1097 Information Sources. *Water Resources Research*.
1098 https://doi.org/10.1029/2017WR021895

1099 O'Loughlin, F. E., Paiva, R. C. D., Durand, M., Alsdorf, D. E., & Bates, P. D. (2016). A
1100 multi-sensor approach towards a global vegetation corrected SRTM DEM product.
1101 *Remote Sensing of Environment*. https://doi.org/10.1016/j.rse.2016.04.018

1102 Paiva, R. C.D., Collischonn, W., Bonnet, M. P., De Gonçalves, L. G. G., Calmant, S.,
1103 Getirana, A., & Santos Da Silva, J. (2013). Assimilating in situ and radar altimetry
1104 data into a large-scale hydrologic-hydrodynamic model for streamflow forecast in
1105 the Amazon. *Hydrology and Earth System Sciences*. https://doi.org/10.5194/hess-
1106 17-2929-2013

1107 Paiva, R. C.D., Collischonn, W., & Tucci, C. E. M. (2011). Large scale hydrologic and
1108 hydrodynamic modeling using limited data and a GIS based approach. *Journal of*
1109 *Hydrology*. https://doi.org/10.1016/j.jhydrol.2011.06.007

1110 Paiva, R. C. D., Buarque, D. C., Collischonn, W., Bonnet, M. P., Frappart, F., Calmant,
1111 S., & Bulhões Mendes, C. A. (2013). Large-scale hydrologic and hydrodynamic
1112 modeling of the Amazon River basin. *Water Resources Research*.
1113 https://doi.org/10.1002/wrcr.20067

1114 Pan, M., & Wood, E. F. (2006). Data assimilation for estimating the terrestrial water
1115 budget using a constrained ensemble Kalman filter. *Journal of Hydrometeorology*.
1116 https://doi.org/10.1175/JHM495.1

1117 Pan, S., Liu, L., Bai, Z., & Xu, Y. P. (2018). Integration of remote sensing
1118 evapotranspiration into multi-objective calibration of distributed hydrology-soil-
1119 vegetation model (DHSVM) in a humid region of China. *Water (Switzerland)*.
1120 https://doi.org/10.3390/w10121841

1121 Pan, S., Pan, N., Tian, H., Friedlingstein, P., Sitch, S., Shi, H., Arora, V.K., Haverd, V.,
1122 Jain, A.K., Kato, E., Lienert, S., Lombardozzi, D., Nabel, J.E.M.S., Ottlé, C.,
1123 Poulter, B., Zaehle, S., Running, S.W. (2020). Evaluation of global terrestrial
1124 evapotranspiration using state-of-the-art approaches in remote sensing, machine
1125 learning and land surface modeling. *Hydrol. Earth Syst. Sci.*
1126 https://doi.org/10.5194/hess-24-1485-2020

1127 Pathiraja, S., Marshall, L., Sharma, A., & Moradkhani, H. (2016). Hydrologic modeling
1128 in dynamic catchments: A data assimilation approach. *Water Resources Research*.
1129 https://doi.org/10.1002/2015WR017192

1130 Pellet, V., Aires, F., Munier, S., Fernández Prieto, D., Jordá, G., Arnoud Dorigo, W., et
1131 al. (2019). Integrating multiple satellite observations into a coherent dataset to
1132 monitor the full water cycle - Application to the Mediterranean region. *Hydrology*
1133 *and Earth System Sciences*. https://doi.org/10.5194/hess-23-465-2019

1134 Peña-Arancibia, J. L., Zhang, Y., Pagendam, D. E., Viney, N. R., Lerat, J., van Dijk, A.
1135 I. J. M., et al. (2015). Streamflow rating uncertainty: Characterisation and impacts
1136 on model calibration and performance. *Environmental Modelling and Software*.
1137 https://doi.org/10.1016/j.envsoft.2014.09.011

1138 Poméon, T., Diekkrüger, B., & Kumar, R. (2018). Computationally efficient
1139 multivariate calibration and validation of a grid-based hydrologic model in sparsely
1140 gauged West African river basins. *Water (Switzerland)*.
1141 https://doi.org/10.3390/w10101418

1142 Pontes, P. R. M., Fan, F. M., Fleischmann, A. S., de Paiva, R. C. D., Buarque, D. C.,
1143 Siqueira, V. A., et al. (2017). MGB-IPH model for hydrological and hydraulic
1144 simulation of large floodplain river systems coupled with open source GIS.
1145 *Environmental Modelling and Software*.
1146 https://doi.org/10.1016/j.envsoft.2017.03.029

1147 Rajib, M. A., Merwade, V., & Yu, Z. (2016). Multi-objective calibration of a hydrologic
1148 model using spatially distributed remotely sensed/in-situ soil moisture. *Journal of*
1149 *Hydrology*. https://doi.org/10.1016/j.jhydrol.2016.02.037

1150 Rakovec, O., Kumar, R., Attinger, S., & Samaniego, L. (2016). Improving the realism
1151 of hydrologic model functioning through multivariate parameter estimation. *Water*
1152 *Resources Research*. https://doi.org/10.1002/2016WR019430

1153 Reichle, R. H., McLaughlin, D. B., & Entekhabi, D. (2002). Hydrologic data

1154 assimilation with the ensemble Kalman filter. *Monthly Weather Review*.
1155 https://doi.org/10.1175/1520-0493(2002)130<0103:HDAWTE>2.0.CO;2

1156 Rosenqvist, A., Shimada, M., Ito, N., & Watanabe, M. (2007). ALOS PALSAR: A
1157 pathfinder mission for global-scale monitoring of the environment. In *IEEE*
1158 *Transactions on Geoscience and Remote Sensing*.
1159 https://doi.org/10.1109/TGRS.2007.901027

1160 Samaniego, L., Kumar, R., & Attinger, S. (2010). Multiscale parameter regionalization
1161 of a grid-based hydrologic model at the mesoscale. *Water Resources Research*.
1162 https://doi.org/10.1029/2008WR007327

1163 Schattan, P., Schwaizer, G., Schöber, J., & Achleitner, S. (2020). The complementary
1164 value of cosmic-ray neutron sensing and snow covered area products for snow
1165 hydrological modelling. *Remote Sensing of Environment.*
1166 https://doi.org/10.1016/j.rse.2019.111603

1167 Schneider, R., Nygaard Godiksen, P., Villadsen, H., Madsen, H., & Bauer-Gottwein, P.
1168 (2017). Application of CryoSat-2 altimetry data for river analysis and modelling.
1169 *Hydrology and Earth System Sciences*. https://doi.org/10.5194/hess-21-751-2017

1170 Schumacher, M., Forootan, E., van Dijk, A. I. J. M., Müller Schmied, H., Crosbie, R. S.,
1171 Kusche, J., & Döll, P. (2018). Improving drought simulations within the Murray-
1172 Darling Basin by combined calibration/assimilation of GRACE data into the
1173 WaterGAP Global Hydrology Model. *Remote Sensing of Environment*.
1174 https://doi.org/10.1016/j.rse.2017.10.029

1175 Semenova, O., & Beven, K. (2015). Barriers to progress in distributed hydrological
1176 modelling. *Hydrological Processes*. https://doi.org/10.1002/hyp.10434

1177 Shafii, M., & Tolson, B. A. (2015). Optimizing hydrological consistency by
1178 incorporating hydrological signatures into model calibration objectives. *Water*
1179 *Resources Research*. https://doi.org/10.1002/2014WR016520

1180 Silvestro, F., Gabellani, S., Rudari, R., Delogu, F., Laiolo, P., & Boni, G. (2015).
1181 Uncertainty reduction and parameter estimation of a distributed hydrological
1182 model with ground and remote-sensing data. *Hydrology and Earth System*
1183 *Sciences*. https://doi.org/10.5194/hess-19-1727-2015

1184 Siqueira, V., Fleischmann, A., Jardim, P., Fan, F., & Collischonn, W. (2016). IPH-
1185 Hydro Tools: a GIS coupled tool for watershed topology acquisition in an open-
1186 source environment. *Revista Brasileira de Recursos Hídricos*.
1187 https://doi.org/10.21168/rbrh.v21n1.p274-287

1188 Siqueira, V. A., Paiva, R. C. D., Fleischmann, A. S., Fan, F. M., Ruhoff, A. L., Pontes,
1189 P. R. M., et al. (2018). Toward continental hydrologic-hydrodynamic modeling in
1190 South America. *Hydrology and Earth System Sciences*.
1191 https://doi.org/10.5194/hess-22-4815-2018

1192 Sivapalan, M., Takeuchi, K., Franks, S. W., Gupta, V. K., Karambiri, H., Lakshmi, V.,
1193 et al. (2003). IAHS Decade on Predictions in Ungauged Basins (PUB), 2003-2012:
1194 Shaping an exciting future for the hydrological sciences. *Hydrological Sciences*
1195 *Journal*. https://doi.org/10.1623/hysj.48.6.857.51421

1196 Sun, W., Ishidaira, H., & Bastola, S. (2012). Calibration of hydrological models in

1197 ungauged basins based on satellite radar altimetry observations of river water level.
1198 *Hydrological Processes*. https://doi.org/10.1002/hyp.8429

1199 Sun, W., Fan, J., Wang, G., Ishidaira, H., Bastola, S., Yu, J., et al. (2018). Calibrating a
1200 hydrological model in a regional river of the Qinghai–Tibet plateau using river
1201 water width determined from high spatial resolution satellite images. *Remote*
1202 *Sensing of Environment*. https://doi.org/10.1016/j.rse.2018.05.020

1203 Sun, W. C., Ishidaira, H., & Bastola, S. (2010). Towards improving river discharge
1204 estimation in ungauged basins: Calibration of rainfall-runoff models based on
1205 satellite observations of river flow width at basin outlet. *Hydrology and Earth*
1206 *System Sciences*. https://doi.org/10.5194/hess-14-2011-2010

1207 Tapley, B. D., Bettadpur, S., Ries, J. C., Thompson, P. F., & Watkins, M. M. (2004).
1208 GRACE measurements of mass variability in the Earth system. *Science*.
1209 https://doi.org/10.1126/science.1099192

1210 Tarpanelli, A., Brocca, L., Melone, F., & Moramarco, T. (2013). Hydraulic modelling
1211 calibration in small rivers by using coarse resolution synthetic aperture radar
1212 imagery. *Hydrological Processes*. https://doi.org/10.1002/hyp.9550

1213 Teutschbein, C., & Seibert, J. (2012). Bias correction of regional climate model
1214 simulations for hydrological climate-change impact studies: Review and evaluation
1215 of different methods. *Journal of Hydrology*.
1216 https://doi.org/10.1016/j.jhydrol.2012.05.052

1217 Vrugt, J. A., Diks, C. G. H., Gupta, H. V., Bouten, W., & Verstraten, J. M. (2005).
1218 Improved treatment of uncertainty in hydrologic modeling: Combining the
1219 strengths of global optimization and data assimilation. *Water Resources Research*.
1220 https://doi.org/10.1029/2004WR003059

1221 Wagener, T., McIntyre, N., Lees, M. J., Wheater, H. S., & Gupta, H. V. (2003).
1222 Towards reduced uncertainty in conceptual rainfall-runoff modelling: Dynamic
1223 identifiability analysis. *Hydrological Processes*. https://doi.org/10.1002/hyp.1135

1224 Wambura, F. J., Dietrich, O., & Lischeid, G. (2018). Improving a distributed
1225 hydrological model using evapotranspiration-related boundary conditions as
1226 additional constraints in a data-scarce river basin. *Hydrological Processes*.
1227 https://doi.org/10.1002/hyp.11453

1228 Werth, S., & Güntner, A. (2010). Calibration analysis for water storage variability of the
1229 global hydrological model WGHM. *Hydrology and Earth System Sciences*. https://
1230 doi.org/10.5194/hess-14-59-2010

1231 Werth, S., Güntner, A., Petrovic, S., & Schmidt, R. (2009). Integration of GRACE mass
1232 variations into a global hydrological model. *Earth and Planetary Science Letters*.
1233 https://doi.org/10.1016/j.epsl.2008.10.021

1234 Willem Vervoort, R., Miechels, S. F., van Ogtrop, F. F., & Guillaume, J. H. A. (2014).
1235 Remotely sensed evapotranspiration to calibrate a lumped conceptual model:
1236 Pitfalls and opportunities. *Journal of Hydrology*.
1237 https://doi.org/10.1016/j.jhydrol.2014.10.034

1238 Winsemius, H. C., G. Savenije, H. H., & M. Bastiaanssen, W. G. (2008). Constraining
1239 model parameters on remotely sensed evaporation: Justification for distribution in

1240 ungauged basins? *Hydrology and Earth System Sciences*.
1241 https://doi.org/10.5194/hess-12-1403-2008

1242 Xu, C. Y., Widén, E., & Halldin, S. (2005). Modelling hydrological consequences of
1243 climate change - Progress and challenges. *Advances in Atmospheric Sciences*.
1244 https://doi.org/10.1007/BF02918679

1245 Xu, X., Li, J., & Tolson, B. A. (2014). Progress in integrating remote sensing data and
1246 hydrologic modeling. *Progress in Physical Geography*.
1247 https://doi.org/10.1177/0309133314536583

1248 Yamazaki, D., Kanae, S., Kim, H., & Oki, T. (2011). A physically based
1249 description of floodplain inundation dynamics in a global river routing
1250 model. *Water Resources Research*. https://doi.org/10.1029/2010WR009726

1251 Yapo, P. O., Gupta, H. V., & Sorooshian, S. (1998). Multi-objective global optimization
1252 for hydrologic models. *Journal of Hydrology*. https://doi.org/10.1016/S0022-
1253 1694(97)00107-8

1254 Zajac, Z., Revilla-Romero, B., Salamon, P., Burek, P., Hirpa, F., & Beck, H. (2017).
1255 The impact of lake and reservoir parameterization on global streamflow
1256 simulation. *Journal of Hydrology*. https://doi.org/10.1016/j.jhydrol.2017.03.022

1257 Zink, M., Mai, J., Cuntz, M., & Samaniego, L. (2018). Conditioning a Hydrologic
1258 Model Using Patterns of Remotely Sensed Land Surface Temperature. *Water*
1259 *Resources Research*. https://doi.org/10.1002/2017WR021346

1260